AD_____

GRANT NUMBER DAMD17-96-1-6028

TITLE: Mechanisms Underlying the Very High Susceptibility of the Immature Mammary Gland to Carcinogenic Initiation

PRINCIPAL INVESTIGATOR: Michael N. Gould, Ph.D.

CONTRACTING ORGANIZATION: University of Wisconsin
Madison, Wisconsin 53706

REPORT DATE: July 1998

TYPE OF REPORT: Annual

PREPARED FOR: Commander
U.S. Army Medical Research and Materiel Command
Fort Detrick, Maryland 21702-5012

REPORT DOCUMENTATION PAGE

Form Approved
OMB No. 0704-0188

1. AGENCY USE ONLY *(Leave blank)*	2. REPORT DATE	3. REPORT TYPE AND DATES COVERED
	July 1998	Annual (1 Jul 97 - 30 Jun 98)

4. TITLE AND SUBTITLE Mechanisms Underlying the Very High Susceptibility of the Immature Mammary Gland to Carcinogenic Initiation

5. FUNDING NUMBERS
DAMD17-96-1-6028

6. AUTHOR(S)
Michael N. Gould, Ph.D.

7. PERFORMING ORGANIZATION NAME(S) AND ADDRESS(ES)
University of Wisconsin
Madison, WI 53706

8. PERFORMING ORGANIZATION REPORT NUMBER

9. SPONSORING/MONITORING AGENCY NAME(S) AND ADDRESS(ES)
Commander
U.S. Army Medical Research and Materiel Command
Fort Detrick, Frederick, Maryland 21702-5012

10. SPONSORING/MONITORING AGENCY REPORT NUMBER

11. SUPPLEMENTARY NOTES

12a. DISTRIBUTION / AVAILABILITY STATEMENT
Approved for public release; distribution unlimited

12b. DISTRIBUTION CODE

13. ABSTRACT *(Maximum 200*

The overall goal of this project remains to explore the toxic effects of physical and chemical carcinogens on the immature mammary gland as compared to these effects on the young adult mammary gland using a rat model. During the second grant year we have: 1) shown that as with radiation, the rat mammary carcinogen NMU is more cytotoxic in the immature *in situ* mammary gland than it is in the mature gland, 2) established the "Big Blue" mutagenesis assay in the laboratory and are in the process of adapting it to the mammary gland, 3) have set up our first long term carcinogenesis study, 4) have established the "Comet assay" for DNA damage in the lab and are adapting it to mammary cells, and 5) have established subtraction libraries to identify genes which are either under or overexpressed in the immature mammary gland. We are currently analyzing members of these libraries. We feel that these studies will help mechanistically define the epidemiological observation in women which suggests that the immature mammary gland is more susceptible to environmental carcinogens than is the adult gland.

14. SUBJECT TERMS Breast Cancer

15. NUMBER OF PAGES
59

16. PRICE CODE

17. SECURITY CLASSIFICATION OF REPORT	18. SECURITY CLASSIFICATION OF THIS PAGE	19. SECURITY CLASSIFICATION OF ABSTRACT	20. LIMITATION OF ABSTRACT
Unclassified	Unclassified	Unclassified	Unlimited

FOREWORD

Opinions, interpretations, conclusions and recommendations are those of the author and are not necessarily endorsed by the U.S. Army.

____ Where copyrighted material is quoted, permission has been obtained to use such material.

____ Where material from documents designated for limited distribution is quoted, permission has been obtained to use the material.

__✓__ Citations of commercial organizations and trade names in this report do not constitute an official Department of Army endorsement or approval of the products or services of these organizations.

__✓__ In conducting research using animals, the investigator(s) adhered to the "Guide for the Care and Use of Laboratory Animals," prepared by the Committee on Care and use of Laboratory Animals of the Institute of Laboratory Resources, national Research Council (NIH Publication No. 86-23, Revised 1985).

____ For the protection of human subjects, the investigator(s) adhered to policies of applicable Federal Law 45 CFR 46.

__✓__ In conducting research utilizing recombinant DNA technology, the investigator(s) adhered to current guidelines promulgated by the National Institutes of Health.

__✓__ In the conduct of research utilizing recombinant DNA, the investigator(s) adhered to the NIH Guidelines for Research Involving Recombinant DNA Molecules.

____ In the conduct of research involving hazardous organisms, the investigator(s) adhered to the CDC-NIH Guide for Biosafety in Microbiological and Biomedical Laboratories.

PI Signature 31 JUL 98 Date

TABLE OF CONTENTS

INTRODUCTION

Our ability to prevent breast cancer by rationally designed intervention requires a better understanding of the etiology of this disease. While the incidence of breast cancer continues to rise, our understanding of the causes underlying both this disease and its increasing incidence are poorly understood. Classical and molecular epidemiology have significantly improved our understanding of the etiology of several cancers such as lung, gastric, head and neck, and bladder. Most epidemiological studies of breast cancer have failed to identify major factors underlying the initiation of breast cancer even though several modifying factors that either promote or inhibit breast cancer development have been identified. A possible explanation for the inability to identify breast cancer initiating agents is suggested by the intensive epidemiological studies of breast cancer etiology in the survivors of the Hiroshima and Nagasaki A-bomb radiation exposures. These studies showed that radiation, even at low doses, causes breast cancer (1). The greatest risk of developing breast cancer was among those exposed when less than ten years of age. The risk of those exposed when 10 to 19 years old was slightly but significantly lower. Risk decreased rapidly with age at exposure thereafter; women over 40 were only minimally susceptible to radiation carcinogenesis (1).

These findings suggest that epidemiological studies that seek environmental and lifestyle factors underlying breast cancer initiation may lose much of their power by restricting their observations to cohorts of middle-aged women (the group that is usually included in most published epidemiological studies). While breast cancer frequently occurs in this middle-aged population, this group of women may have only a minimal sensitivity to the various environmental agents under study, and breast cancer initiation is likely to have occurred decades earlier under a very different environment/lifestyle than is current for this older cohort of women. In addition to studies of radiation carcinogenesis of A-bomb survivors, similar age versus risk trends have been reported in both medically irradiated patients (2), and in several epidemiological studies of cigarette smokers (3). For example, Brinton et al. report an increased relative risk to breast cancer in women who began smoking before age 17 (3). This is consistent with our in vitro studies with primary cultures of human breast epithelial cells in which we demonstrated the genotoxicity of cigarette smoke condensates (4).

Since the first reports of the strong dependence of age at exposure to radiation on breast cancer risk, its importance has been widely recognized; however, its underlying mechanism remains obscure. Before the current epidemiological data set became available, it was only clear that younger females were more susceptible to breast cancer initiation than older women. Accordingly, it was speculated that susceptibility was related to breast development and specifically to the increased rate of parenchymal cell division during breast maturation in the teenage girl. This hypothesis is supported by the data of Russo et al. (5) that shows that susceptibility to DMBA-induced mammary cancer in rats occurs at a period of high breast cell division as the rat becomes sexually mature. In contrast, the most recent epidemiological analysis includes cancers detected in A-bomb survivors through 1985 and shows that the age at exposure for maximum risk of breast cancer initiation by radiation is before puberty and the accompanying menarchal increase in breast cell mitosis (1). Thus the full data set suggests that some aspect of the biology of the immature human breast results in maximal sensitivity to breast cancer initiation. It should also be kept in mind that while the immature breast is most susceptible to breast cancer initiation, the maturing breast (teens to early 20's) is more susceptible

to initiation than the breast of middle-aged, pre-menopausal women. This intermediate sensitivity may be rooted in the increased mitotic rate of the maturing breast parenchyma. Thus at least two physiologic processes may underlie susceptibility to breast cancer initiation: that associated with the immature breast and that associated with the developing breast. The literature has provided little to explain the former observation mechanistically; however, we have recently generated a novel hypothesis that may explain it.

We have shown that the breast stem-cells of sexually immature rats are highly sensitive to the cytotoxic effects of ionizing radiation (6). This sensitivity decreases and then disappears as the rats begin to mature (6). These data have led to our central hypothesis that the inability of the mammary parenchyma of the immature rat to recover from radiogenic cellular damage may underlie an increased susceptibility to radiation-induced genetic lesions that lead to the genesis of breast cancer. It is further hypothesized that this sensitivity to radiation can be extended to other environmental agents. Defining and characterizing the role of the high radiosensitivity of the immature mammary gland in a rat model will provide key data for future studies to assess interspecies extrapolation to women.

Sensitivity to Radiation Cytotoxicity of Mammary Cells as a Function of Age

In order to investigate the effect of age on radiation sensitivity, we irradiated rats at various ages ranging from 1 through 12 weeks of age and assayed their mammary clonogenic (stem) cells' survival. When immature rats were irradiated with 5 Gy (500 rad) when 1, 2, 3 or 4 weeks of age, 10% of the mammary cells survived. In contrast, a 3-fold increase in survival of irradiated mammary cells was observed when mature rats at 8 or 12 weeks of age were irradiated. When complete radiation dose versus cell survival curves were generated, not only did we confirm the quantitative difference in survival of mammary cells from immature and mature rats at all doses tested, but we also found a qualitative difference in the shapes of the survival curves between pre-pubescent and post-pubescent rats. Mammary cell survival curves from irradiated 2- and 4- week-old rats were straight on a semilog plot, indicating a purely exponential cell killing. In contrast, survival curves of mammary cells from 8-week-old rats had an initial shoulder region followed by a terminal exponential portion more typical of mammalian cells. The most common explanation for an initial convex shoulder on a survival curve suggests that it reflects an ability of the cells to recover from low to moderate doses of radiation. It may be further speculated that since the major damage leading to cell death following radiation is damage to DNA, this recovery may consist of DNA damage repair. In addition to cell death, nonrepaired or misrepaired DNA damage can lead directly to mutation and thus indirectly to neoplastic transformation. It is thus speculated that the extremely high sensitivity of the immature human breast to radiation carcinogenesis may result from an increased accumulation of damaged DNA due to a diminished ability to correctly repair DNA damage.

A second period of increased sensitivity may also occur during sexual maturation and gland development. This period of intermediate sensitivity in women may be related to an increased mitotic rate during gland growth at sexual maturation (5).

The relative importance of the two periods of increased sensitivity to breast cancer susceptibility may be species dependent. In order to have the greatest chance of correlating the human and rat results, this proposal will focus on the period of highest sensitivity in the human: the immature gland. We will extend our initial observation of increased radiation sensitivity on cell killing during a homologous period in the rat and test the endpoints of DNA damage,

mutagenesis and carcinogenesis. We will also investigate possible molecular mechanisms underlying the increased radiation sensitivity of the immature mammary parenchyma.

Mechanisms Underlying Radiation Sensitivity of the Immature Mammary Gland

Knowledge of the cellular and molecular biology underlying radiation damage has been expanding rapidly over the last several years. Our group has found that epidermal growth factor (EGF) can modulate radiation sensitivity. We have shown that in two human primary epithelial cell culture systems, breast (7) and prostate (8), the removal of epidermal growth factor from a defined growth medium before and during radiation increases the radiation sensitivity of both cell types. This effect has been shown to be independent of proliferation status (7,8). Others have shown that the removal of EGF inhibits the repair of radiation DNA strand breakage (9).

The in situ mammary gland produces both EGF and transforming growth factor α (TGFα) which signal through the same receptor. However, it is suggested on the basis of cellular and glandular distribution that only TGFα acts within the parenchyma of the gland via an autocrine/paracrine mechanism, whereas EGF is often apically secreted and not locally active (10). In elegant studies, TGFα mRNA was not found to be present in the immature mouse mammary gland; however, it is readily detectable in the maturing gland and persists in the adult virgin gland (10).

We hypothesize that the lack of TGFα in the immature gland leads to the observed increased radiation sensitivity that could extend to mutagenic and oncogenic sensitivity in this immature tissue. We plan to test this hypothesis directly as well as to further explore alternative molecular mechanisms underlying this age- dependent increased radiation sensitivity in the mammary gland.

Establishing the cellular and molecular mechanism underlying the increased sensitivity of the immature breast to carcinogenic environmental exposures will possibly lead to better designs for breast cancer epidemiological studies and to new prevention strategies. For example, if we show that it is likely that the radiation sensitivity of the immature breast extends to chemical xenobiotics then it would suggest that epidemiological studies seeking agents that initiate breast cancer focus on young girls. Secondly, for example, if we demonstrated that this increased sensitivity of the immature breast is due to a low level of mammary gland associated TGFα then this would suggest new pharmacologic breast cancer prevention approaches using either TGFα or preferably non-peptide small molecules with TGFα activity.

PURPOSE

The overall goal of this proposal is to explore the hypothesis that the diminished ability of mammary cells from immature rats to recover from cytotoxic radiation damage may extend to an increased susceptibility to mammary carcinogenesis. If so, such a mechanism may also underlie the observation that the immature breast of pre-pubescent human females is the developmental stage most highly susceptible to breast cancer initiation.

SPECIFIC AIMS

In order to achieve our overall goals, we will address the following specific questions using a rat model:

1. Does the sensitivity to cell killing by ionizing radiation in immature glands extend to various classes of xenobiotic chemical carcinogens including those acting via bulky adducts (DMBA) and alkylating small adducts (NMU)?
2. Does the irradiation of cells from immature mammary glands (in contrast to mature glands) result in a higher sensitivity to the induction of specific locus mutations? Is the spectrum of mutations different in cells from immature and mature glands?
3. Is the immature gland more sensitive to the scopal carcinogenic effect of radiation?
4. Does irradiation of the immature gland (in contrast to the mature gland) result in a) more extensive DNA damage, b) more poorly repaired damage, or c) a greater induction of apoptotic cell death?
5. Is the lack of TGFα production by cells of the immature mammary gland related to the increased sensitivity of radiation-induced cell killing?

How is the spectrum of gene expression in the immature and mature mammary glands different with regard to genes which could directly or indirectly confer altered cellular recovery capacity following cytotoxic and genotoxic damage?

REFERENCES

1. Tokunaga, M., Land, C.E., Yamamoto, T., Asano, M., Tokuoka, S., Ezaki, H. and Nishimori, I. Incidence of female breast cancer among atomic bomb survivors, Hiroshima and Nagasaki, 1950-1980. Radiat. Res. 112:243-272, 1987.
2. Hancock, S.L., Tucker, M.A. and Hoppe, R.T. Breast cancer after treatment of Hodgkin's disease. J. Natl. Cancer Inst. 85:25-31, 1993.
3. Brinton, L.A., Schairer, C., Stanford, J.L. and Hoover, R.N. Cigarette smoking and breast cancer. Am. J. Epidemiol. 123:614-622, 1986.
4. Eldridge, S.R., Gould, M.N. and Butterworth, B.E. Genotoxicity of environmental agents in human mammary epithelial cells. Cancer Res. 52:5617-5621, 1992.
5. Russo, J., Wilgus, G. and Russo, I.H. Susceptibility of the mammary gland to carcinogenesis: I. Differentiation of the mammary gland as determinant of tumor incidence and type of lesion. Am. J. Pathol. 96:721-736, 1979.
6. Shimada, Y., Yasukawa-Barnes, J., Kim, R.Y., Gould, M.N. and Clifton, K.H. Age and radiation sensitivity of rat mammary clonogenic cells. Radiat. Res. 137:118-123, 1994.
7. Howard, S.P., Groch, K.M., Lindstrom, M.J., Wolberg, W.H. and Gould, M.N. Survival of irradiated normal and malignant human mammary epithelial cells under differing growth conditions. In preparation, 1998.
8. Howard, S.P., Groch, K.M., Messing, E.M. and Gould, M.N. Proliferation independent growth factor modulation of human prostate cell radiation sensitivity. Radiat. Res. 143:229-233, 1995.

9. Bildin, V.N., Seregina, T.B. and Zhestyanikov, V.D. Effect of epidermal growth factor (EGF) and insulin on the kinetics of radiation-induced DNA lesions repair. Acta Biol. Hung. 41:51-56, 1990.
10. Snedeker, S.M., Brown, D.F. and DiAugustine, R.P. Expression and functional properties of transforming growth factor α and epidermal growth factor during mouse mammary gland ductal morphogenesis. Proc. Nathl. Acad. Sci. USA 88:276-280,1991.

Year Two: Progress Report

Aim 1: Does the sensitivity to cell killing by ionizing radiation in immature glands extend to various classes of xenobiotic chemical carcinogens including those acting via bulky adducts (DMBA) and alkylating small adducts (NMU)?

In vivo cytotoxicity of 3 versus 8 week old F344 mammary gland following exposure to either NMU or DMBA

Materials and Methods

Animals

Virus-free F344 female and male rats were obtained from Harlan Sprague-Dawley, Inc. (Indianapolis, IN). The breeding of the rats to create 3 week old F344 female donor rats was performed at our facility. All other F344 female rats were obtained directly from Harlan Sprague-Dawley, Inc. All rats were provided with Teklad Lab Blox chow (Harlan Teklad, Madison, WI) and acidified water ad libitum. The rats were housed under a 12 hour light and 12 hour dark cycle.

Carcinogen Treatment

At either 3 or 8 weeks of age, F344 female rats (n=2-5 rats) were treated with either N-nitroso-N-methylurea (NMU) or 7,12-dimethylbenz[*a*]anthracene (DMBA). The NMU was given as a single tail-vein injection at a dose of 80 mg/kg body weight. The NMU was dissolved in 10mg/ml acidified saline, pH 5.0 with acetic acid. The DMBA was administered as a single gastric intubation at a dose of 80 mg/kg body weight. The DMBA was prepared in 20 mg/ml sesame oil, heated in boiling water until dissolved and cooled to room temperature prior to administration.

Mammary Cell Transplantation Assay

Twenty-four hours after carcinogen treatment, the inguinal mammary fat pads of the treated, donor rats were excised following removal of all lymph nodes, and placed into a dish containing DMEM medium (Gibco, Grand Island, NY). The tissue was scissor minced and transferred into a flask containing collagenase (Worthington; type III, 200 mg/ml). After a two hour digestion at 37°C, DNase (Sigma; 7.5 units/ml) was added to each flask and the digestion continued for an additional 15 minutes. Following centrifugation, the cell pellet was washed and further digested

with 0.05% trypsin and 0.02% EDTA for 10 minutes at 37°C. The cells were again pelleted, washed and resuspended for filtration. The cell suspension was filtered through 53μ nylon mesh and the mammary cells in the filtrate were collected, washed, resuspended and counted using a hemocytometer. The cell suspension was serially diluted 1:1 in media. To each of the final dilutions, a equal volume of 50% rat brain homogenate was added. A volume of 0.06 mls of each of the cell dilutions was injected into three sites in the interscapular white fat pad of 8-10 week old recipient rats. These recipient rats had received grafts 2 weeks before transplantation of the pituitary tumor MtT-F4, which induces the transplanted mammary cells to grow and differentiate. At 3 weeks after the transplantation of the mammary cells, the interscapular fat pads were removed, fixed, stained with alum carmine and examined using a dissecting microscope for the development of alveolar units.

The percentages of transplantation sites with an alveolar unit(s) identified was calculated for each cell dilution. This data was fit to the transplantation model of Porter et al. to give an alveolar dose 50% of AD_{50} (1). An AD_{50} is defined as the number of cells per injection required to produce at least one alveolar growth in 50% of the graft sites. This number can then be used to determine the frequency of clonogenic stem-like cells or the clonogenic fraction in the cell suspension (2,3). Clonogen survival following carcinogen exposure is estimated by dividing the value of the AD_{50} of the control, non-treated group by the AD_{50} of the treated group.

Results

	Control		NMU		DMBA	
F344 donor mammary gland	AD_{50}	Clonogen Survival	AD_{50}	Clonogen Survival	AD_{50}	Clonogen Survival
3 week - a	549	x	2046	27%	nd	nd
3 week - b	306	x	1034	30%	489	63%
8 week - a	322	x	529	61%	516	62%
8 week - b	372	x	555	67%	516	72%

The current results obtained from the cell transplantation assays may be seen in the table above. It appears that the clonogen survival frequency of 8 week old F344 mammary glands exposed to either 80 mg/kg NMU or DMBA for 24 hours is ~60-70%. This same frequency of clonogen survival is observed in 3 week old F344 mammary glands exposed to DMBA; however, NMU treatment of 3 week old F344 mammary gland shows an increase in cytotoxic effect, resulting in a clonogen survival frequency of ~30%. Another experiment is currently underway to confirm the findings regarding the cytotoxic effects of NMU and DMBA on 3 week old F344 mammary gland. We speculate that NMU, a direct acting carcinogen, and DMBA, an indirect acting carcinogen, exert their cytotoxic effects by different molecular mechanisms. The current results suggest 8 week old mammary gland exposed to either NMU or DMBA and 3 week old mammary gland exposed to DMBA are capable of equivalent levels of repair. In contrast, it is possible that the mammary gland of the 3 week old rats lacks an appropriate repair system to correct the damage caused by the NMU as compared to the 8 week old rats treated with NMU and 3 week old rats treated with DMBA.

References

1. Porter, EH, Hewitt, HB, and Blake, ER. The transplantation kinetics of tumor cells. Br J Cancer, 27:55-62, 1973.
1. Gould, MN, Biel, WF and Clifton, KH. Morphological and quantitative studies of gland formation from inocula of monodispersed rat mammary cells. Exp Cell Res, 107:405-416, 1977.
2. Clifton, KH, and Gould, MN. Clonogen transplantation assay of mammary and thyroid epithelial cells. In: CS Potten and JH Hendry (eds.), Cell Clones: Manual of Mammary Cell Techniques, pp.128-138. New York: Churchhill Livingstone, 1985.

Aim 2: Does the irradiation of cells from immature mammary glands (in contrast to mature glands) result in a higher sensitivity to the induction of specific locus mutations? Is the spectrum of mutations different in cells from immature and mature glands?

The purpose of this aim is to determine whether the spectrum of ionizing radiation-induced mutations produced in the immature and mature rat mammary gland differs, possibly accounting for the differential survival of the rat mammary epithelial cells (RMECs). Previous work on this aim was severely limited by the failure of Stratagene's products to perform as expected. First, considerable time was spent trying to find a bacterial agar that would allow detection of the blue mutant plaques. After that was successfully completed, further work involved finding a DNA isolation method that would allow isolation of genomic rat mammary epithelial cell DNA suitable for the Big Blue assay.

In the last update, it was proposed that in order to test the Big Blue system in the laboratory, Big Blue rats would be dosed with ethylnitrosourea, a known potent mammary mutagen. After further consideration, it was decided that this would not be the most effective test, since as a chemical carcinogen, it would be expected to produce a different spectrum of mutations than radiation. Instead, it was determined that a more appropriate test would be to replicate the results of a paper which screened for and characterized spleen mutations from ionizing radiation-treated mice (Winegar, *et al.* 1994). Although the paper reported results obtained from males, the experiment in our laboratory was conducted on both male (to most closely mimic conditions reported) and female mice, from which organoids could be isolated and analyzed in addition to spleen. This paper was chosen because it was the only published report of the Big Blue system being used to analyze ionizing radiation-induced mutations.

Three doses of ionizing radiation were tested in the experiment (I517): 0 Gy, 1 Gy, and 3 Gy, all with a 14 day expression period. The Winegar group had performed the 0 Gy and 1 Gy experiments; the 3 Gy experiment was added in order to increase the likelihood that mutations would be produced. Difficulties arose during the spleen DNA isolation procedure; the precipitated proteins did not form a tight pellet in the bottom of the tube after centrifugation. Additional steps were taken in an attempt to separate the protein from the supernatant, but upon spectrophotometric analysis of the DNA, it was clear that these steps had failed. Both the purity and concentration of the DNA were unacceptable for use in the assay.

The DNA isolation procedure was repeated using additional frozen spleen. The concentration and purity were not substantially improved, but it was decided to continue with the assay because considerable effort and expense had already been incurred. The animals had

been dosed and sacrificed. The large plates, which would become unusable before another experiment could be conducted, were already poured. Instead of obtaining no information, even a little bit of insight would be useful.

The DNA was packaged and pre-titered according to the Big Blue instruction manual. The number of plaques produced was lower than the number expected, but it was assumed that this problem was due to the poor quality of the DNA.

The first issue in the data analysis was to determine the total number of plaques plated, since that figure is essential in determining the mutant frequency. Two methods, the 5 Squares method and the dilution plate method, are available for calculating the total number of plaques plated. Using the 5 Squares method, on each of two experimental plates, five squares are drawn using a template purchased from Stratagene. The plaques in the squares are counted, an average is taken, and the total number of plaques is calculated. The dilution plate method involves producing a dilution of the packaging reaction, which is then plated. The plaques on the plates are counted, and the total number of plaques plated is calculated. If both methods are used, they should agree within 10% of each other. Both methods were used in this experiment (I517) but they did not consistently agree within 10% of each other, as shown in Figure 1. The mutant frequencies were calculated with all of the total plaque values, as can be seen in Figure 2.

Although it is known that the males were irradiated, it appears from the mutant frequencies calculated that the irradiation did not have an effect on the males. The females, however, did show increasing damage with increasing dose, although the values were lower than those obtained for male mice by the Winegar group. The control male mouse had mutant frequencies greater than those obtained by the Winegar group, while the female control mouse DNA did not produce a mutant plaque. However, these problems could be attributed to the small number of plaques obtained. For example, a hypothetical mutant frequency, based on the presence of one mutant plaque, was calculated for the female control animal; by all calculation methods, the value was within the range of the mutant frequencies obtained for the male animals but above the expected value.

The results from the females analyzed in this experiment were promising. A positive dose-response was obtained for the females. However, it was not determined why the males, which were expected to have higher mutant frequencies, did not replicate the Winegar, *et al.* results. Also, the DNA yield and purity were still below acceptable levels.

The experiment was repeated (I705) using the remaining spleen samples and fresh plates. The same problem occurred with the DNA isolation procedure. After consulting with one of the scientists in the laboratory, it was revealed that this problem was not unique to the Big Blue DNA isolation; the cause was the failure of the microcentrifuges to spin hard enough to pellet the precipitated proteins. However, this was discovered too late to improve this experiment, and the DNA concentrations were far below the recommended concentration for use in the packaging reaction. It was learned from the Stratagene technical service line that although it was not optimal, it was possible to use a larger volume of less concentrated DNA in the packaging reaction. Since this was the last of the DNA, making it the last opportunity to obtain any data from these spleens, it was determined to package all the DNA isolated in this experiment. There was also DNA left from the last isolation; it was packaged, as well. Finally, in order to check the packaging efficiency of the packaging reaction, control DNA was packaged in parallel with the spleen DNA.

The spleen DNA produced far fewer plaques than necessary for a statistically significant mutant frequency to be determined. This was thought to be due to the poor quality and

concentration of the DNA. However, the control DNA only produced $2.25x10^8$ plaque forming units/μg of DNA, which is less than the guaranteed value of $1.0x10^9$ plaque forming units/μg of DNA. This was attributed to the age of the control lambda DNA or the use of the chloroform to preserve the packaging reaction overnight.

Total plaques plated as determined by the calculation method are shown in Figure 3, and the mutant frequencies determined from those values are shown in Figure 4. Although the DNA isolated in the previous experiment showed similar mutant frequency trends in the females, the values for the males were not consistent with the previous results. The male values from the older DNA also did not match the values obtained using the newly isolated DNA, so the older DNA values were not considered to be reliable. If only the newly isolated DNA values are examined, this experiment more closely replicates the results obtained by the Winegar group. The males irradiated with 1 Gy showed higher mutant frequencies than both the expected value and the 3 Gy-irradiated male. However, it was promising that the 1 Gy-irradiated male mutant frequencies regardless of calculation method agreed well with the published values. The female values also correlated well with the values published by the Winegar group. These results were interpreted as an indication that the system functioned well in the females. Also, there must have been an error made during the packaging procedure in the previous experiment, since the mutant frequencies from the male DNA more closely resembled the expected values in this experiment. Again, the nonirradiated rats showed higher mutant frequencies than expected, but this is likely due to the small number of plaques analyzed. It was determined that the Big Blue system can be utilized successfully in the laboratory.

Another conclusion that can be extrapolated to all other Big Blue experiments was drawn from this experiment. The total number of plaques plated will be determined by taking the average of the 5 Squares method performed on two plates. This method is better than the dilution method because the 5 Squares method is performed on the actual experimental plates. Not only are additional plates not needed, but also this method accounts for the state of the experimental plates. The dilution method involves an additional dilution step, as well as the pouring of an additional plate(s). The dilutions can introduce errors due to inaccurate pipetting or liquid clinging to the pipettor tip. In addition, the cost of the materials required to pour an additional dilution plate(s), as well as the time involved to prepare additional plates and dilutions, are not justified, considering that the 5 Squares Method is more accurate.

The next step (I744) was to verify the mutant plaques produced in the previous two experiments. The mutant plaques and one non-mutant plaque from each plate from which a mutant was found were cored and replated. Briefly, the plaque of interest is cored using a sterilized glass pipette. It is incubated overnight in SM buffer supplemented with chloroform to allow the phage to elute from the agar plug. Fresh plating bacteria are infected with the eluted phage and replated. This step is essential because there are a number of artifacts that can appear to be mutants in the experimental plates. True mutants when replated will produce all blue plaques. On the original experimental plate, a bacterial colony can appear to be a plaque. After coring and storage with chloroform, which kills bacteria but not phage, a bacterial colony will not replate; there will be a lawn of bacteria, but no plaques. Pinpoint mutants and ex-vivo mutations are another problem; when replated, these will produce a combination of clear and blue plaques. To be stringent, mutant frequencies can only be based on "mutant" plaques that produce greater than 50% blue plaques upon replating. The Winegar group did not perform the verification step, so there could be no comparison made with published results. The verification procedure was successful; corrected mutant frequencies are shown in Figure 5.

The next step, which was performed by the Winegar group, was mutant characterization (I757). Cored plaques from the verification plates were processed using the Big Blue DNA Excision Kit, which isolates the pLIZ plasmid. The plasmids can then be isolated using minipreps. In this initial experiment, the miniprep kit used was Stratagene's Clear-Cut Miniprep Kit. Concentrations and purities of DNA isolated using this kit were unacceptable, even after multiple optimizations. Also unsuccessful were minipreps using Qiagen's QIAprep Spin Plasmid Kit and modifications of it. Even repeating the plasmid isolation procedure from the Big Blue DNA Excision Kit to produce new starting material for the minipreps was not successful. Finally, the Wizard Miniprep Kit produced DNA of the desired purity and concentration. Restriction digestions performed according to the protocol reported by the Winegar group, although successful, did not reveal any visible deletions or insertions; this indicates that the mutants were caused by point mutations which could not be detected by agarose gel electrophoresis.

Next, the mammary epithelial organoids isolated from the mice, as well as organoids that had been frozen from Big Blue rats, were analyzed. Because the mouse organoid pellets were so small, there was a very limited amount of DNA isolated from them. The rat organiod pellets were a little larger, and they produced more DNA. Using a different microcentrifuge than the one previously used, the purity of the DNA was superior to that previously isolated. Rat spleen DNA collected from the same rats from which the organoids were isolated was also analyzed. Control DNA was packaged in parallel to test the Transpack efficiency. The total number of plaques produced by the experimental samples was again insufficient for any statistically significant argument. The control DNA plates did not show any plaques at all on two platings, indicating that the Transpack was not packaging the DNA efficiently. The Transpack was to blame for the insufficient number of plaques produced.

The final experiment (K55) conducted during this update period was designed to produce a dose-response curve in RMECs from mature glands exposed to ionizing radiation. Before this was done, the new Transpack sent by Stratagene to replace the defective Transpack was tested and found to perform up to the guaranteed level. Two females were exposed to 10 Gy, two were exposed to 5 Gy, and two unexposed animals served as negative controls. All were to have a 14-day expression period following irradiation, but the 10 Gy-exposed rats were found dead on the eleventh day. Because 10 Gy was above the $LD_{50/30}$, the animals were observed daily. They appeared healthy on day 9, but were not checked on day 10. As soon as it was known that the animals were dead, their organoids were isolated, and their other tissues were collected. The remaining four animals were sacrificed on the 14^{th} day post-irradiation, and tissues were collected. DNA was then isolated, packaged, and plated.

Figure 6 shows the total plaques plated, and Figure 7 shows the calculated mutant frequencies. The mutant plaques have not yet been verified. No mutants were found in the control animals. From this experiment, all that can be concluded for the mammary gland background mutant frequency is that it is less than 1.40×10^{-4}. (The other control animal had a mutant frequency of less than 8.06×10^{-5}.) No mutants were found in one of the 5 Gy-irradiated rats, but the other 5 Gy-irradiated rat did produce one mutant plaque that appears to be truly a mutant. Both 10 Gy-exposed animals produced mutants. However, as can be seen in Figure 6, the total number of plaques plated per animal falls far short of statistical significance.

This very preliminary experiment indicates that detecting radiation-induced mutations, especially those produced by low doses, in the mammary gland may be problematic. This may be because the system is not optimal for detecting the large-scale deletions expected from ionizing

radiation.

N-nitroso-N-methylurea (NMU), an alkylating agent, has been found (See Aim 1) to also produce age-dependent cell killing in RMECs similar to that produced by ionizing radiation. Since NMU is an alkylating agent, mutations produced by it are more likely to be detected in the Big Blue system. NMU has been used in conjunction with an electromagnetic field in the Big Blue rat embryo fibroblast line (Suri, *et al.* 1996).

Another similar alkylating agent, ethylnitrosourea (ENU), has been used in the same cell line and was found to produce detectable mutations (Zimmer, *et al.* 1996). ENU was also found to produce mutations in the splenic T cells of male Big Blue mice (Walker, *et al.* 1996 and Skopek, *et al.* 1995).

Therefore, Big Blue studies will shift from ionizing radiation-induced mutations to NMU-induced mutations. Since ENU and NMU produce different spectra of mutations and the DNA adducts produced by NMU are shorter-lived than those produced by ENU, the protocols will have to be optimized for NMU (Swanson, *et al.* 1996). Initial studies will involve determining the optimal dose of NMU that can be tolerated, particularly by the immature rats. Once those preliminary studies are completed, the experiments will be conducted initially on the immature rats, which are expected to be more sensitive than the mature rats. Other tissues will be analyzed concurrently with the mammary cells to determine whether the system can detect mutations in the mammary cells. If it is found that the system will efficiently detect NMU-induced RMEC mutations, then the radiation studies will resume. If, however, the system will detect NMU-induced mutations in other organs but not RMECs, then another method of determining differential mutations will have to be devised.

References

Skopek, T.R., Kort, K.L., and Marino, D.R. Relative sensitivity of the endogenous hprt gene and lacI transgene in ENU-treated Big Blue B6C3F1 mice. *Environmental and Molecular Mutagenesis* 26(1): 9-15, 1995.

Swanson, S.M., Guzman, R.C., Tsukamoto, T., Huang, T.T., Dougherty, C.D., and Nandi, S. N-ethyl-n-nitrosourea induces mammary cancers in the pituitary-isografted mouse which are histologically and genotypically distinct from those induced by N-methyl-N-nitrosourea, *Cancer Letters* 102(1-2): 159-65, 1996.

Suri, A., deBoer, J., Kusser, W., and Glickman, B.W. A 3 milliTesla 60 Hz magnetic field is neither mutagenic nor co-mutagenic in the presence of menadione and MNU in a transgenic rat cell line. *Mutation Research* 372(1): 23-31, 1996.

Walker, V.E., Gorelick, N.J., Andrews, J.L., Craft, T.R., deBoer, J.G., Glickman, B.W., and Skopek, T.R. Frequency and spectrum of ethylnitrosourea-induced mutation at the hprt and lacI loci in splenic lymphocytes of exposed lacI transgenic mice. *Cancer Research* 56 (20): 4654-61, 1996.

Winegar, R.A., Lutze, L.H., Hamer, A.D., O'Loughlin, K.G., and Mirsalis, J.C. Radiation-induced point mutations, deletions and micronuclei in *lacI* transgenic mice. *Mutation Research* 307: 479-487, 1994.

Zimmer, D.M., Zhang, X.B., Harbach, P.R., Mayo, J.K., and Aaron, C.S. Spontaneous and ethylnitrosourea-induced mutation fixation and molecular spectr at the lacI transgene in the Big Blue rat-2 embryo cell line. *Environmental and Molecular Mutagenesis* 28(4): 325-33, 1996.

Figure 1: Total Plaques by Calculation Method (I517)

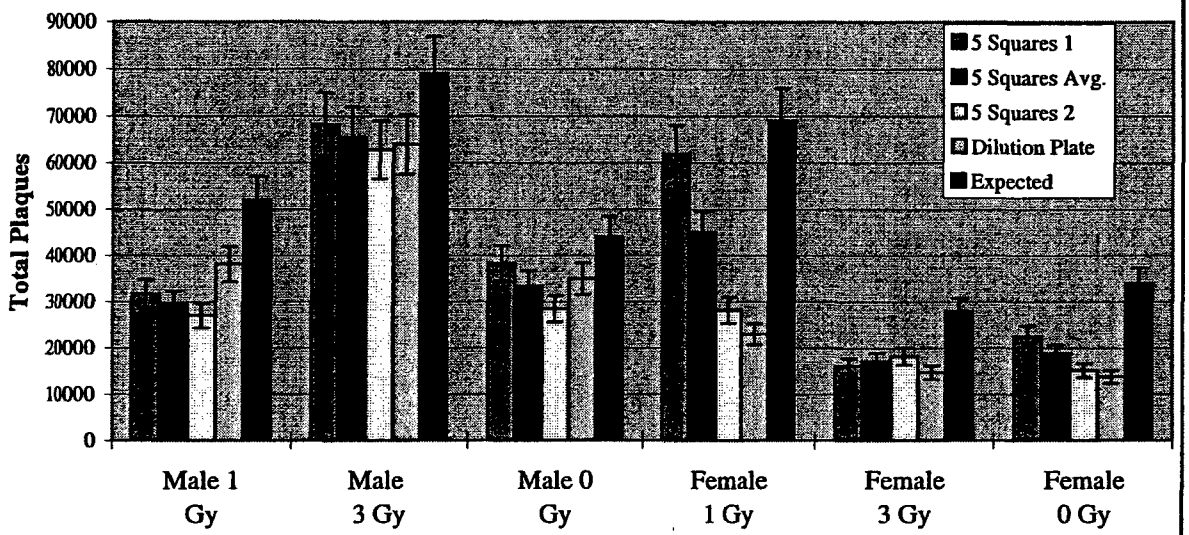

Error bars, which represent 10% of the bar's value, are shown to illustrate how well the values for each sample agree with each other. Expected values were determined from the pretiter.

Figure 2: Mutant Frequencies by Calculation Method (I517)

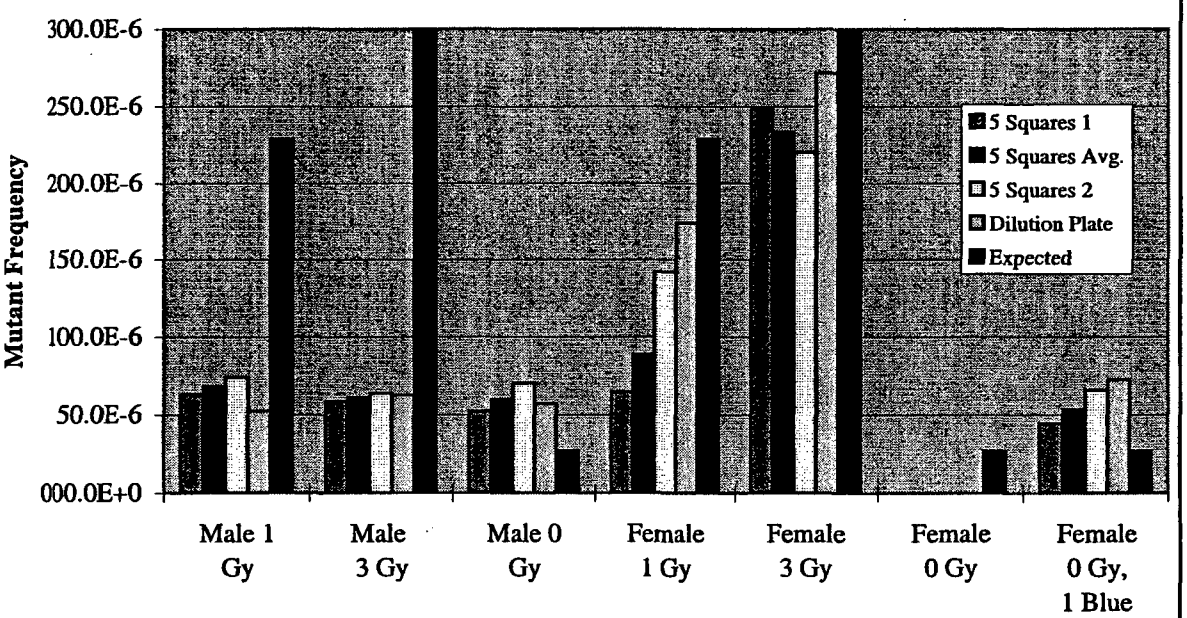

It can be seen that the mutant frequencies vary with the method used to calculate the total number of plaques plated. Additionally, since no blue plaques were found on the Female 0 Gy plates, the calculated mutant frequency was 0. The mutant frequency was calculated as if there had been one mutant plaque; this drove the values over the expected value. Thus, the small number of total plaques made it impossible to find the expected mutant frequency. Expected values are from Winegar, *et al.*

Figure 3: Total Plaques by Calcuation Method (I705)

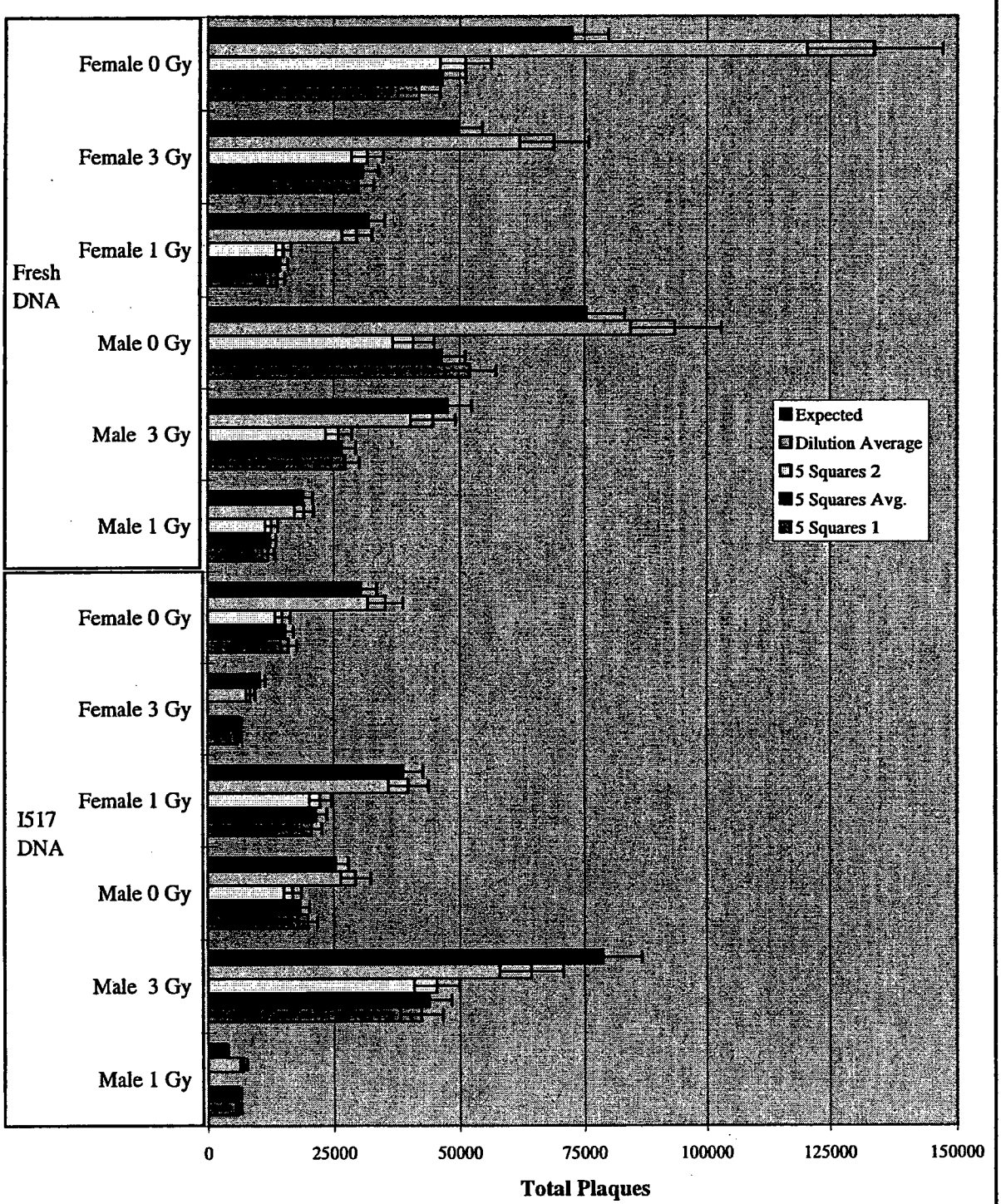

Error bars, which represent 10% of the value of the bar, are shown to illustrate how well the calculation methods agree with each other. Expected values are from the pretiter.

Figure 4: Mutant Frequencies by Calculation Method (I705)

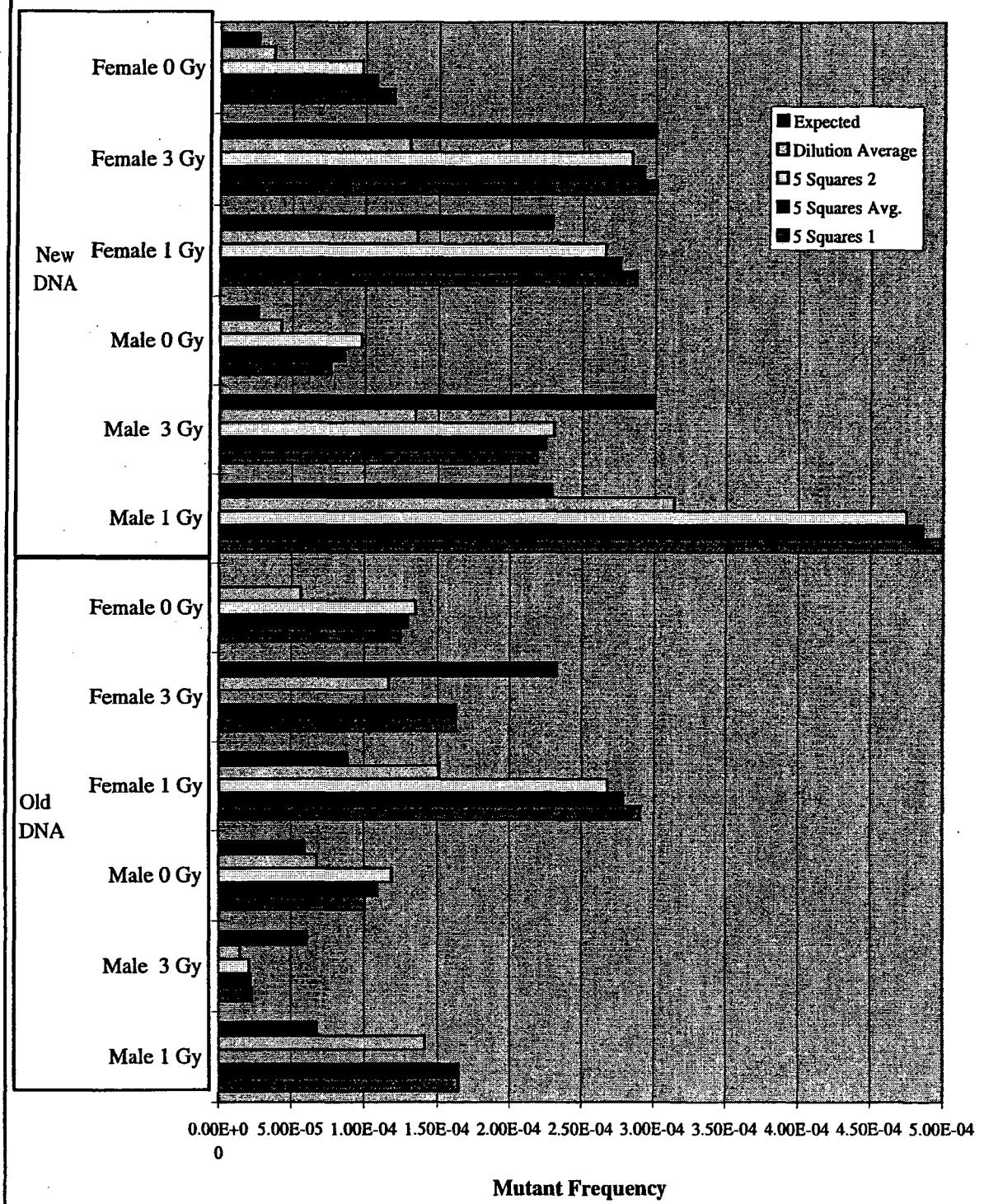

Expected values for the mutant frequencies from the Old DNAare the mutant frequencies from the previous plating with that DNA calculated by the 5 Squares Average method. Expected values for the mutant frequencies from the New DNA are from Winegar, *et al.*

Figure 5: Corrected Mutant Frequencies

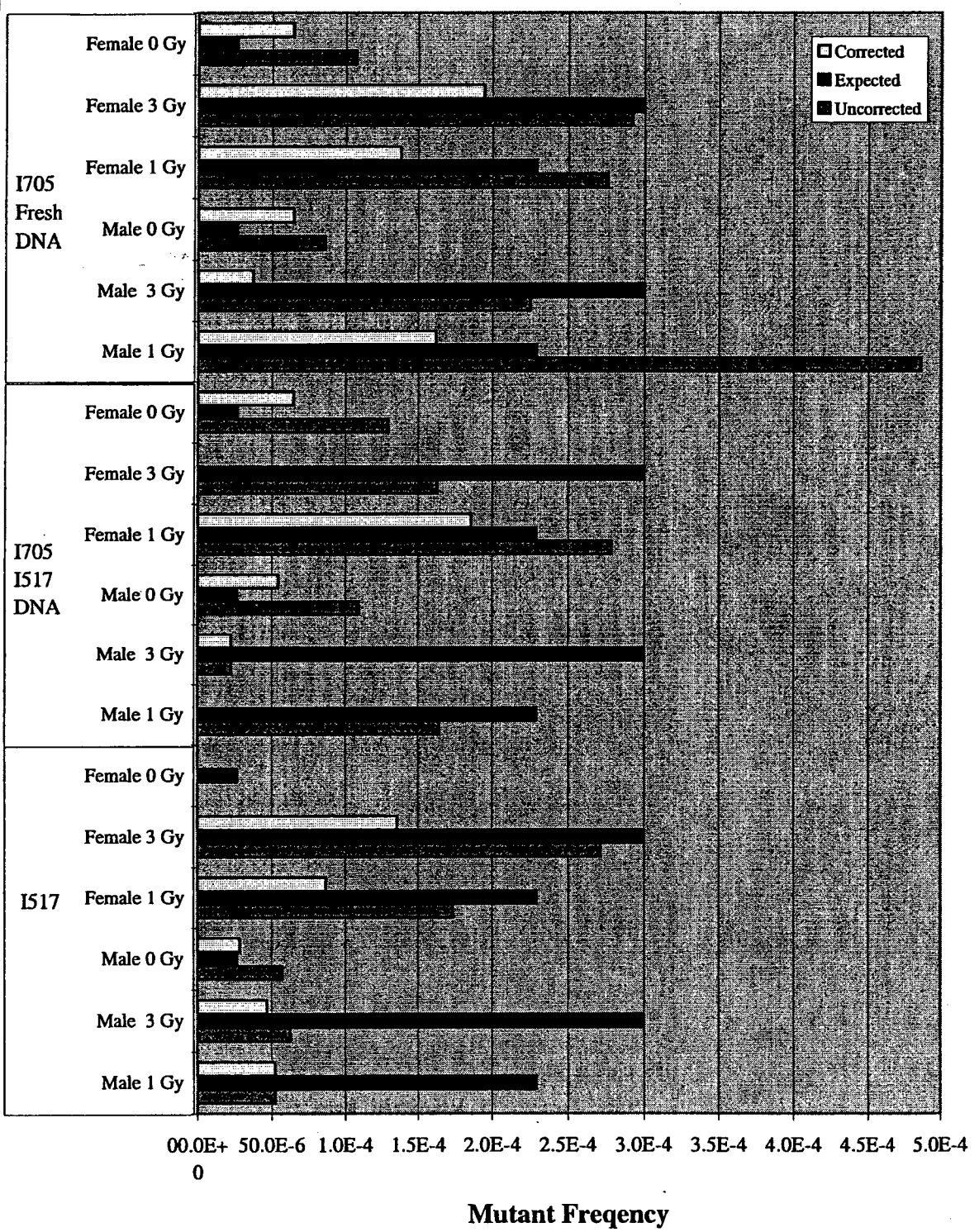

Corrected values ranged from 0% to 100% of the uncorrected values. Expected values are those reported by Winegar, *et al.*

Figure 6: K55 Total Plaques Plated

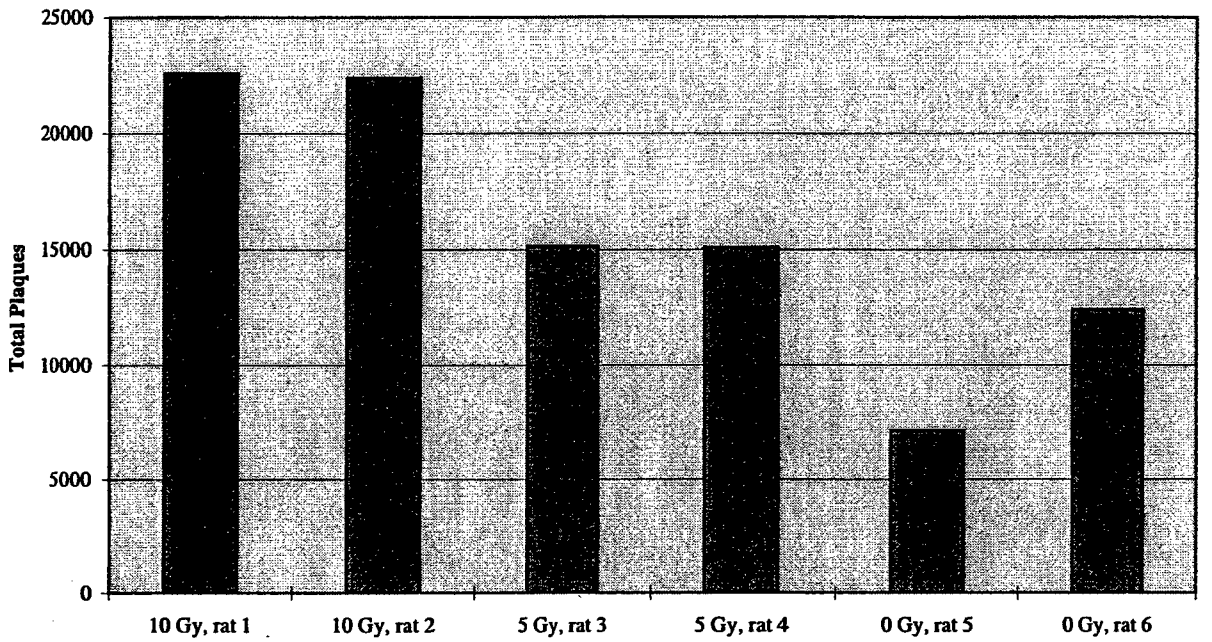

The total number of plaques plated is far too low to be able to make any statistically significant conclusions. More platings of the DNA will be required. It is not known whether, as it appears, the dose had a significant effect on the total number of plaques plated.

Figure 7: K55 Mutant Frequencies

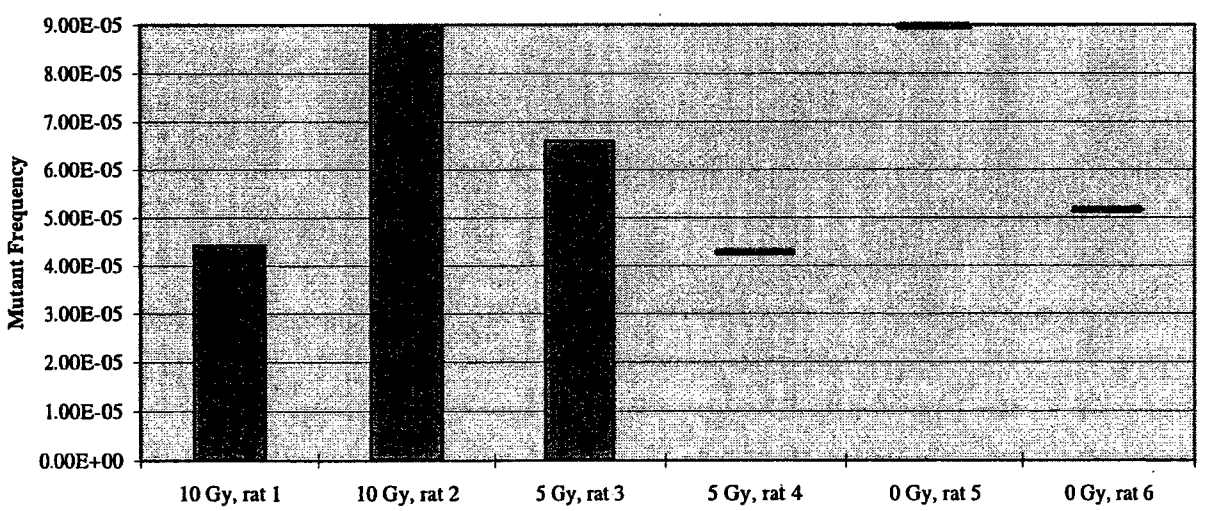

The values shown for rats 1, 2, and 3 are the unverified mutant frequencies actually observed. The values shown for rats 4, 5, and 6 are the hypothetical values that would have been calculated had one mutant plaque been observed; these are the maximum possible mutant frequencies. No significant dose-response was observed, except that the 0 Gy animals had no mutants.

Aim 3: Is the immature gland more sensitive than the mature gland to the scopal carcinogenic effect of radiation?

The purpose of this aim is to determine if the immature rat mammary gland in an intact 3 week old F344 rat is more sensitive to radiation-induced carcinogenesis than is the mature rat mammary gland in an intact 8 week old F344 rat.

Dosimetry: Anesthetized rats were irradiated with 6 Mev electrons from a Clinac 2300 medical linear accelerator. The rats were laid supine on the treatment couch and placed into a collimated radiation field from the bottom of their ears to the anus. A. 1.5 cm thick slab of bolus (tissue equivalent material) was placed over their skin to reduce the range of the electrons into the body and to protect the ovaries. The top surface of the bolus was set at 100cm from the target of the accelerator.
Anesthetized intact rats were laid supine on a flat surface and measurements were taken (maximum length from rat's chin to anus, maximum width across rat and average distance from skin surface of rat to surface at location of ovaries). These measurements were taken for several rats in each age group. The mammary glands were assumed to extend to a depth of 0.5cm beneath the skin surface. The machine was programmed to deliver 2.5 Gy at a 2 cm depth. With the 1.5 cm bolus in place, this is 0.5 cm depth beneath the rat's skin. Because the dose decreases with depth, the tissue toward the skin received a higher dose. The maximum dose to the rat was calculated to be 3.2 Gy at the skin surface. The ovaries of the smallest rat (the smallest rat's ovaries would receive the highest dose) would receive a calculated dose of 12% of 2.5 Gy, or 0.3 Gy.
To verify the dose received, two animals from each age group were irradiated as above after TLD's were inserted at 6 locations/rat (RB and LB, RD and LD, one at each ovary). The TLD's were read using a Victoreen Thermoluminescence Dosimeter Reader (Model 2800), normalized to a calibration standard exposed at the same time as the animals and the resulting micro Coulombs were converted into Gy (dose received).

Rat of Age x	Location of TLD	mCoulombs (average)	Dose in Gy (average)
3 week old	RB	5.95	3.23
3 week old	LB	5.85	3.18
3 week old	RD	5.59	3.04
3 week old	LD	NR	NR
3 week old	R ovary	NR	NR
3 week old	L ovary	3.61	1.95
8 week old	RB	4.14	2.25
8 week old	LB	4.84	2.63
8 week old	RD	4.25	2.31
8 week old	LD	4.56	2.48
8 week old	R ovary	2.38	1.29
8 week old	L ovary	1.87	1.02

NR=Not Reportable, TLD's were not readable due to moisture absorbed

Highest dose to mammary gland measured was 3.23 Gy, highest dose calculated was 3.2 Gy. Highest dose to ovaries measured was 1.95 Gy, highest dose calculated was .3 Gy.

Results:
The first mammary carcinoma (2 in one animal) was detected at 30 weeks post-irradiation in the 8 week old animal group. As of 42 weeks post-irradiation, no other tumors have arisen in any of the groups. This is not unexpected in that most radiation induced mammary tumors arise at ≥ 12 months post-irradiation.

		8 week old control	8 week old 2.5 Gy	3 week old 2.5 Gy
	# animals/group	36	31	31
Wks 0-28 post-irrad	Total tumors/group	0	0	0
Wks 0-28 post-irrad	Ave tumors/animal	0	0	0
Week 30 post-irrad	Total tumors/group	0	2	0
Week 30 post-irrad	Ave tumors/animal	0	.06	0
Week 42 post-irrad	Total tumors/group	0	2	0
Week 42 post-irrad	Ave tumors/animal	0	.06	0

Aim 4: Does irradiation of the immature gland (in contrast to the mature gland) result in a) more extensive DNA damage, b) more poorly repaired damage, or c) a greater induction of apoptotic cell death?

The purpose of this aim is to determine whether the age-differential survival of irradiated rat mammary epithelial cells (RMECs) is due to differing amounts of DNA strand breaks realized or repaired by the two ages of animals. The work completed prior to this year all involved performing the comet assay on V79 cells in order to become familiar with the procedure. It was discovered that media must be present during irradiation in order for detectable damage to occur.

The first experiments performed during this period characterized the effect of irradiation in the presence of media. Although the neutral comet assay results did not improve (Figures 1 and 2) the alkaline assay results were more promising (I392). As can be seen in Figure 1, although the histograms are tight and normal, they are all clustered in the same region, not shifting to the right with increasing dose, as would be expected. Figure 2 illustrates that the median tail moment in the neutral comet assay actually decreases with increasing dose. Figure 3 shows the histograms from the alkaline assay. These are also tight, normal histograms, and they do show

increasing damage, as illustrated in Figure 4 where the median tail moments are plotted with dose. It is interesting to note in Figure 3 how the tailing at higher tail moments increases with dose, indicating that there is a population of cells undergoing more damage than the majority of the cells.

However, the presence of media during irradiation of the cells did not fully correct for the problem of the lack of a linear dose-response. The neutral assay has the inverse of the expected relationship. In addition, although the dose response curve is linear with a positive slope above 4 Gy, there is actually a decrease in median tail moment between the 0 and 4 Gy points.

Conversations with Dr. Ben Nelms, who developed the software for the assay in our laboratory, revealed that the line of V79 cells being used in these experiments can give unusual results in this assay. It was suggested that an alternate V79 cell-line be used. The next experiments (I401) were conducted with freshly prepared cells of the alternative line. Additionally, higher doses of irradiation were used to increase the probability that an effect would be seen. Figure 5 shows that the alkaline assay was able to detect increasing damage with increasing dose; this is also seen in Figure 6, where the median tail moments from the alkaline and neutral assays are plotted. There was a positive dose-response in the alkaline assay, but the neutral assay again revealed a negative dose-response. The histograms in Figure 7 reiterate this pattern, as they do not shift to the right like the alkaline histograms do.

At this point, a literature review revealed a significant oversight in the performance of the irradiations for the comet assays. Significant DNA damage repair could occur within the first 15 minutes after irradiation unless steps are taken to block that repair; the most common non-chemical method is to irradiate the cells on ice and keep them on ice after irradiation. The next experiments (I438 and I444) were performed in this manner. Again, higher doses were used in order to maximize any damage. Once the procedure is established, it can be optimized for sensitivity at lower doses. The comet assay was performed and repeated, with the alkaline results corresponding well. The histograms from the alkaline assay are shown in Figure 8. They were normal and illustrated increasing damage with increasing dose. The neutral histograms did not show as large an increase in damage with dose, but there was a subtle trend of increasing damage with increasing dose as evidenced by a slight shift in the histogram to the right. (Figure 9). Figure 10 shows the median tail moments from the two experiments. The alkaline assays had a positive dose-response, and were successfully replicated. The neutral trends for the first time were also positive, but the curves did not overlap as well as the alkaline median tail moment curves. Also, the neutral assay was not as sensitive as the alkaline.

The goal of the next experiment (I446) was to optimize the neutral assay. Conditions that could be adjusted included the lysis and electrophoresis conditions. Conceptually, the conditions had to be adjusted so that if there were double-strand breaks, the resulting DNA fragments could be more effectively electrophoresed into the tail. Thus, the detergent concentration in the lysis buffer was increased in order to facilitate more complete membrane degradation so that there would be less of a barrier to the electrophoretic mobility of the DNA. Additionally, a higher voltage was applied during electrophoresis to more strongly pull the damaged fragments into the tail. Figure 11 is a tree diagram illustrating the way that the new conditions were tested. The histograms for all slides were acceptable, and the median tail moment trends are shown in Figure 12.

Conditions A and C showed a positive trend, while conditions B and D showed a negative trend with increasing dose. It is hypothesized that the negative trend exhibited by conditions B and D was artifactual. The higher voltage could have resulted in such extreme migration of the

DNA fragments that they could not all be analyzed by the image capture and analysis software. It was not practical to further enlarge the analysis window because of the interference caused by overlapping comets. The failure to analyze the most mobile fragments would in this system result in the appearance of a decreasing trend, since the largest tail moments are calculated for the cells from which the majority of the fragments have migrated the farthest. Since the most damaged (and furthest migrated) fragments were hypothetically outside the analysis window, this would lead to a severe underestimation of the tail moment. Condition C (normal electrophoresis, harsher lysis) showed the best dose-response curve in this experiment. The slope of the dose-response curve was positive, it was the most linear of the dose-response curves, and the 0 Gy median tail moment (background) was the lowest. However, the error bars still overlapped; more sensitivity is desired.

The next experiment (I557) expanded on what was learned in the previous experiment. Figure 13 is a tree diagram indicting the conditions tested. The previous experiment indicated that increased lysis would improve results, and that higher voltage during electrophoresis impaired them. In this experiment, the detergent concentration was further increased to increase lysis. Instead of increasing the voltage, the duration of electrophoresis was increased. Figure 14 shows the median tail moment trends. Increased electrophoresis time did increase sensitivity, particularly at higher doses, without creating the negative trend artifact. However, the error bars still overlapped.

At this point it was determined that the principles of the assay were well understood. Further optimization of conditions would only be specific to V79 cells, and would not be useful toward the goal of performing the assay on primary rat mammary epithelial cells (RMECs). Further efforts were directed toward optimizing the assay conditions for primary RMECs.

The initial effort (I819) did not meet with success. The primary rat mammary epithelial cells were isolated according to procedures standard in this laboratory. It appeared that the organoids were attaching and behaving normally. Before the assay could be performed, though, the cultures became contaminated. It was later determined that the "contamination" problem experienced in the lab at this time was not in fact bacterial contamination; instead, it was precipitated protein.

Another literature search revealed a recent paper which employed the comet assay to study human mammary epithelial cells (Martin, *et al.* 1997). The conditions used in that paper were substantially different from the conditions that had been used on the V79 cells. Particularly, the lysis solution contained more detergent. Primary RMECs were isolated and cultured (I1015). The five dishes were to be treated with irradiation in different ways in order to determine the most effective way to dose the cells. First, one dish was not irradiated, and served as the negative control. One dish of cells was irradiated (on ice, with medium) with 5 Gy, while another was irradiated (on ice, with medium) with 10 Gy. These dishes were then trypsinized and processed through the comet assay. Two more dishes were trypsinized to produce a cell suspension, which was irradiated on ice with either 5 Gy or 10 Gy before being processed through the comet assay. The cells from all treatment conditions remained firmly attached to the dishes even with the trypsin treatment and had to be powerwashed off the dish with the trypsin solution. The cells were allowed to lyse overnight in the cold room, and the unwinding step was conducted in the cold room for three hours in electrophoresis buffer with no buffer changes. The slides were electrophoresed and stained with propidium iodide (PI). Upon microscopic examination, no cells were visible on either 10 Gy slide; only the control and 5 Gy slides could be analyzed. Figure 15 shows the histograms created from these slides. They reveal that the assay was not successful.

The histograms are not tight or normal; in fact, it almost appears that there are two distinct populations of cells in each treatment condition. It appeared that trypsinization prior to irradiation produced more damage than irradiation prior to trypsinization. Of significance is the control slide's histogram, which reveals that there is considerable background damage. The control slide's histogram is not significantly different from the histogram of the 5 Gy pre-trypsin treatment.

This wide distribution of tail moments, with many in the high range, could likely be due to the way the cells were treated. The long exposure to the 0.1% trypsin, although it did not remove the cells from the dish, could have harmed the cells. The powerwashing could also have damaged the cells. Finally, the overnight lysis step could have been too harsh. These problems could also have accounted for the disappearance of the 10 Gy-treated cells; the cells could have been too damaged before they were embedded in the agarose, so their DNA could have already leaked out of the cell.

These problems were addressed in the next experiment (K16). New primary RMECs were isolated and cultured in T75 flasks instead of dishes in order to allow rougher agitation with the trypsin . Trypsinization was not more successful in this experiment; the cells still remained attached to the plastic even after rough shaking. The cells that did become dislodged were counted and diluted in PBS for slide preparation before irradiation on ice. The cells were kept on ice until irradiation approximately 2 hours later. Doses used were 2.5 Gy, 5 Gy, and 10 Gy (in addition to nonirradiated controls). Table 1 is a scheme showing how the slides were treated. Histograms are shown in Figure 16. In many of the slides, there again appeared to be two distinct populations of cells; unfortunately, this phenomenon was again observed in the 0 Gy control slides, indicating that the background damage was again too high. This could be due to the difficulties with the trypsinization. There were cells visible in the 10 Gy-treated cells, indicating that it is possible to analyze such cells; the overnight lysis could have been the problem. However, the 10 Gy-treated cells demonstrated less damage than the control cells. Further optimization is necessary.

The next experiment (K25) addressed the trypsinization issue. First, stronger trypsin was used (0.25% instead of 0.1%). Second, it was discovered that the trypsin aliquots used in our lab did not contain EDTA, which had to be added to the thawed trypsin. That step was taken in this experiment. Other steps to be optimized were the unwinding and electrophoresis time, as well as irradiation in PBS or media. It was decided that the assay should be developed with irradiation of adherent cells instead of suspensions because future repair studies would require that the cells be adherent after irradiation. Figure 17 shows the treatment scheme. Trypsinization was performed at room temperature immediately from the irradiation. The histograms (not shown) became much more normal, although some still exhibited the possibility of two distinct populations of cells. Median tail moments with treatment are shown in Figure 18. From this experiment, it appeared that the stronger trypsin with the added EDTA did improve the background damage problem, although further improvement is desirable. Another possible way to reduce the background damage would be to reduce the time that the cells sit in suspension, albeit on ice, before being embedded in the agarose and processed. Finally, from this experiment, it appears that the best conditions as yet tested are a 40-minute unwinding, followed by 30 or 35 minutes of electrophoresis. It is unclear whether irradiation with PBS or media is better.

The last comet experiment (K47) conducted during the update period further addressed the trypsinization issue and additional optimization of conditions. Figure 19 illustrates the scheme of conditions used in this experiment. For the first time, the agarose concentration was tested.

Again, unwinding and electrophoresis times were tested, as was irradiation with PBS or media. In this experiment, the trypsinization procedure was radically altered. Again, 0.25% trypsin, supplemented with EDTA was used. However, the PBS used for the washes (to remove media prior to trypsinization) was calcium- and magnesium-free because those ions can interfere with the trypsin. Two washes of trypsin were used; the cells were incubated at 37°C after the second wash had been removed, leaving a thin film of trypsin on the cells. The dishes were checked periodically under the microscope and tapped to dislodge the cells. Media was added to inactivate the trypsin when the cells had become dislodged. This was the most effective procedure yet for removing the cells from the dish. When the cell dilutions were prepared and the cells were mixed with the agarose, gentle vortexing was employed to ensure complete mixing. The histograms (not shown) varied by treatment. Some showed the possible two populations of cells; these histograms were generally not very tight. Other histograms, however, showed the desired tight normal distribution. Figure 20 shows the median tail moment histograms produced for all the treatment conditions, and Figure 21 shows the histograms from the treatment conditions that produced the best dose-response. These conditions were determined to be the best because they showed the best separation between the control cells and the 5 Gy-irradiated cells.

Further optimization is still necessary. The control cells could still potentially be composed of two populations, as revealed by the histograms (Figure 21). This could be a result of the delay between dilution and slide preparation/lysis. This should be corrected when smaller-scale experiments are conducted with fewer conditions to test. Additionally, the procedure can be staggered so that the cells are processed immediately by condition; this would limit the time that the dilutions sit on ice. Another problem is the failure of the 10 Gy-irradiated cells to show greater damage than the 5 Gy-irradiated cells. This could also be the result of the extended period of time that the cells spend on ice. If the "second" population of cells (the ones with the higher median tail moments) seen in the histogram of the control slide is truly produced by damage suffered while the cells are on ice, then all the of cells should be experiencing the same damage. The population of cells most susceptible to that damage would likely be the cells that are already most damaged by irradiation. It is possible, then, that the most damaged cells (the ones that should be radically shifting the histogram to the right in the 10 Gy-treated cells) are being killed - even lysed to the point that they spill their DNA. This would render them invisible in the assay, and artificially shift the tail moment histogram to the left, as is seen. In fact, this is a concern whenever higher doses of irradiation produce median tail moments less than those produced by lower doses; the most damaged cells are so damaged that they do not maintain their integrity long enough to be analyzed.

Future experiments are planned to further optimize the alkaline comet assay. A smaller scale experiment will test the conditions determined in the previous experiment to be the most effective. The time that the cells are on ice between trypsinization and agarose-embedding will be minimized to attempt to lower the background damage and increase the high-dose damage. One higher dose will be included to determine whether the high-dose problem is really a damage plateau. Once that is determined, then a transplantation assay can be performed in conjunction with a comet assay to determine whether the conditions used (irradiating the cells in culture instead of irradiating intact animals) will mimic the differential survival observed when intact animals are irradiated. If the transplantation assay reveals the same phenomenon, then the optimized conditions will be used in a series of comet assays.

References

Martin, F.L., Venitt, S., Carmichael, P.L., Crofton-Sleigh, C., Stone, E.M., Cole, K.J., Gusterson, B.A., Grover, P.L., and Phillips, D.H. DNA damage in breast epithelial cells: detection by the single-cell gel (comet) assay and induction by human mammary lipid extracts. *Carcinogenesis.* 18(12): 2299-2305. 1997.

Figure 1: I392 Neutral Comet Assay Tail Moment Histograms

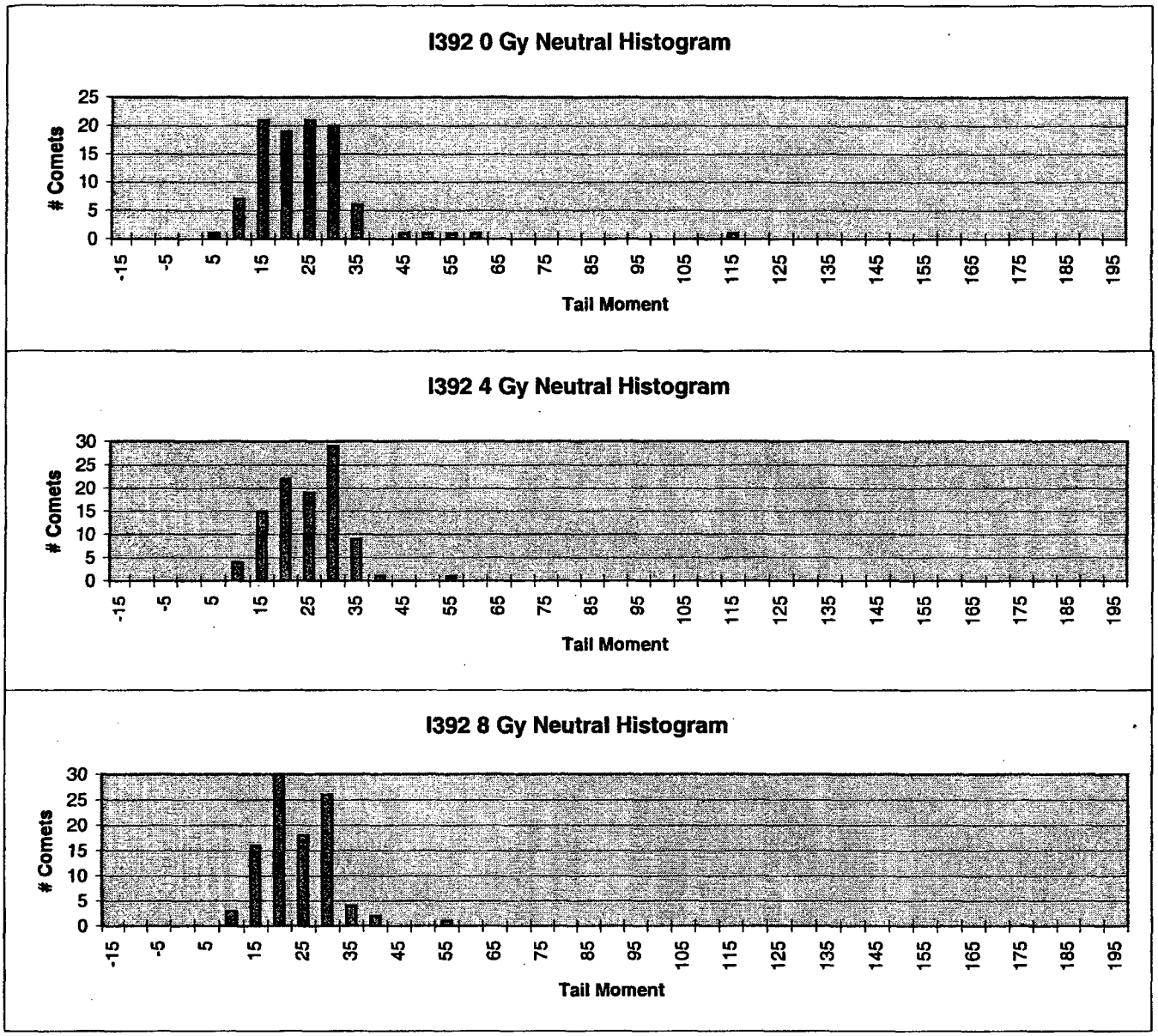

There is no 12 Gy neutral histogram
because the gel fell off
the 12 Gy neutral slide.

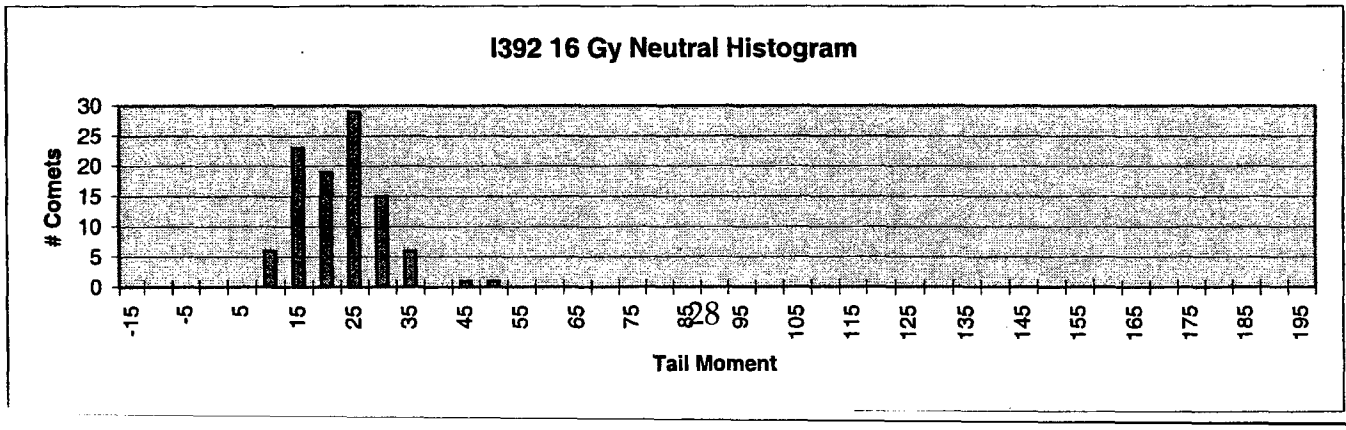

Figure 2: I392 Neutral Comet AssayMedian Tail Moment Trend

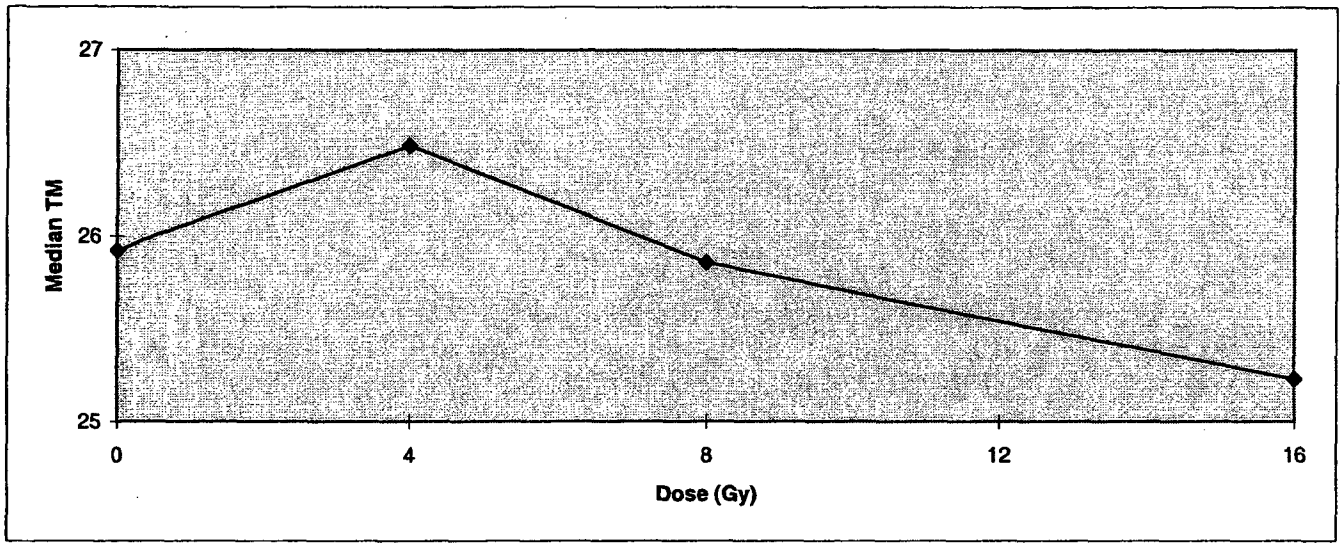

Figure 3: I392 Alkaline Comet Assay Median Tail Moment Trend

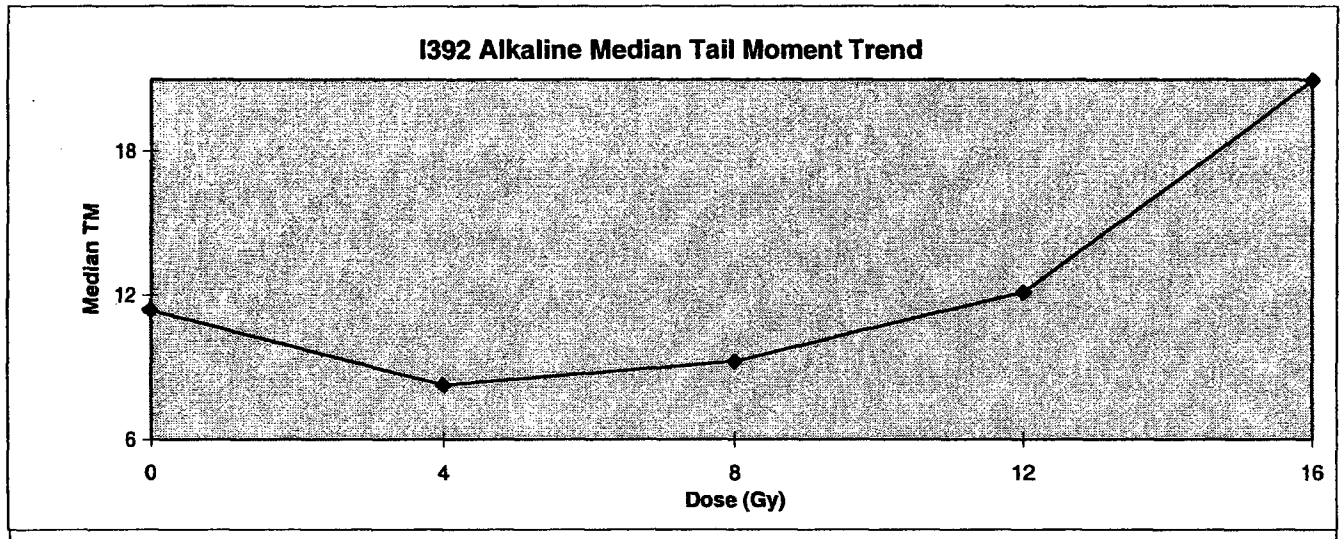

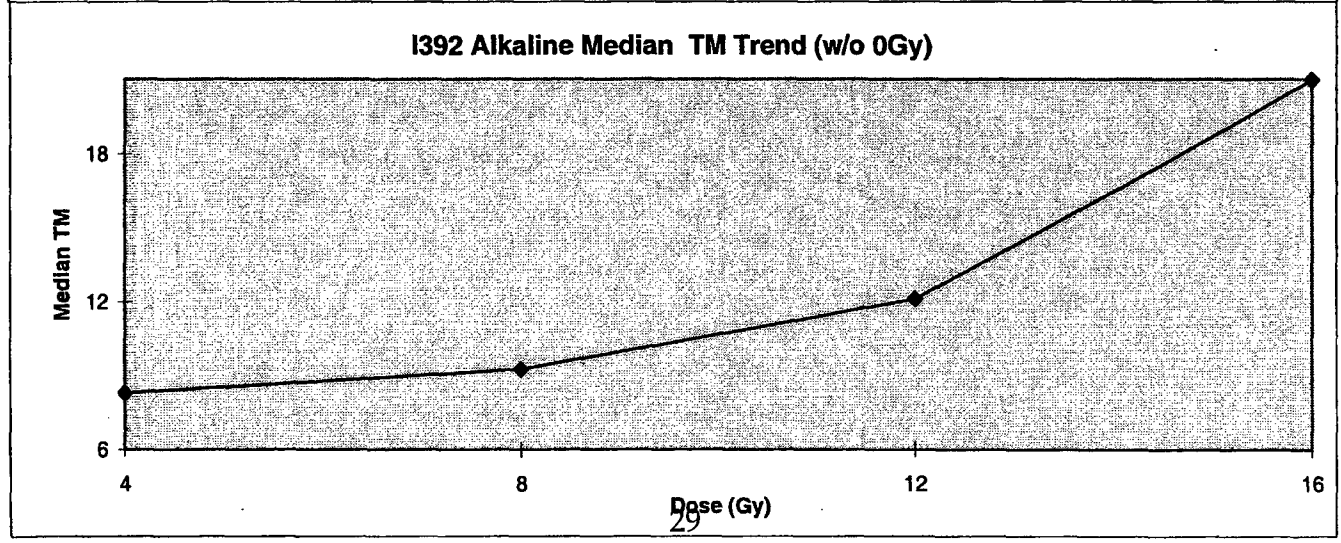

Figure 4: I392 Alkaline Comet Assay Tail Moment Histograms

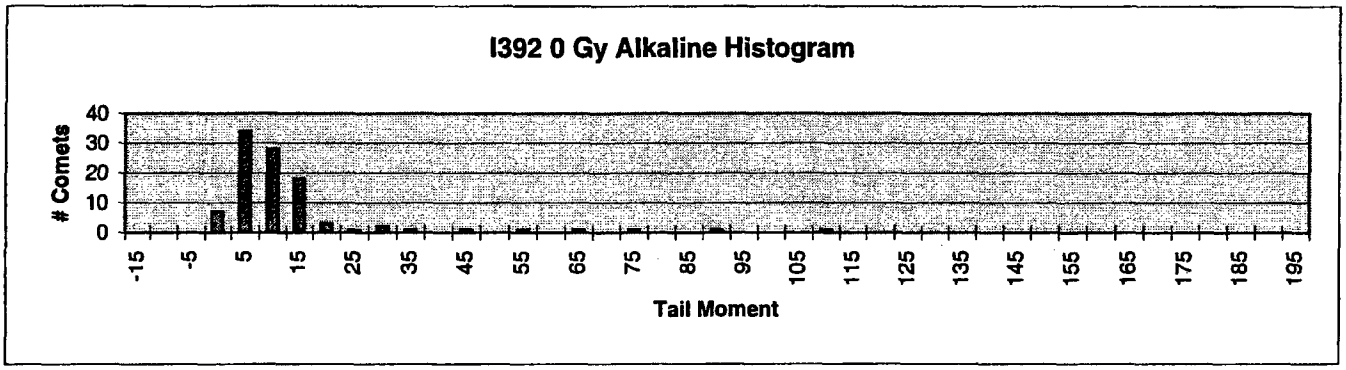

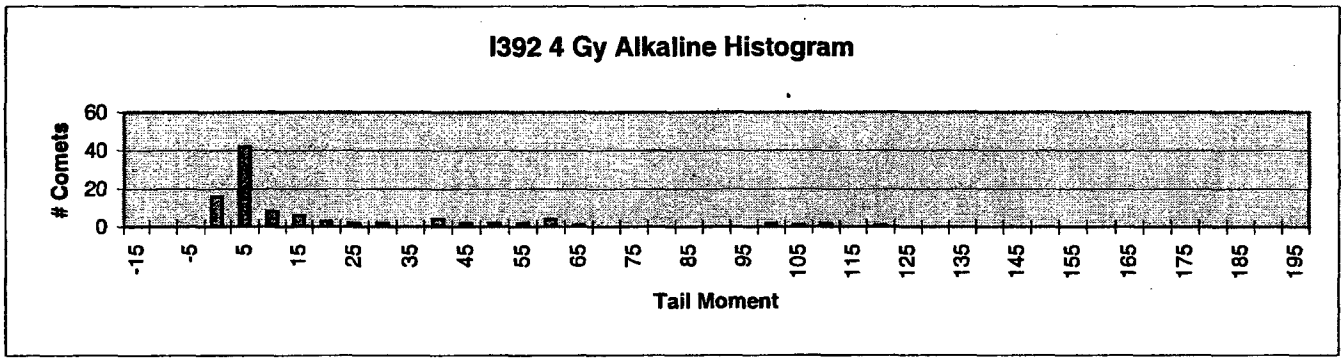

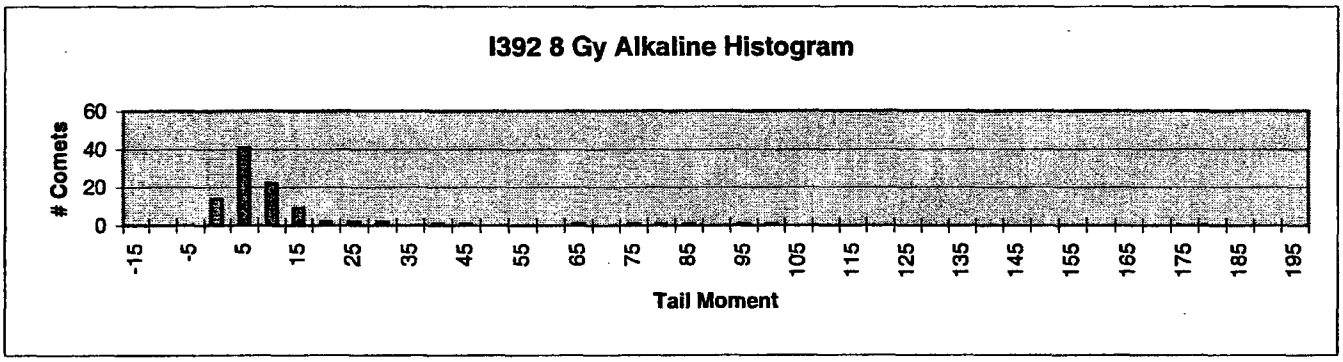

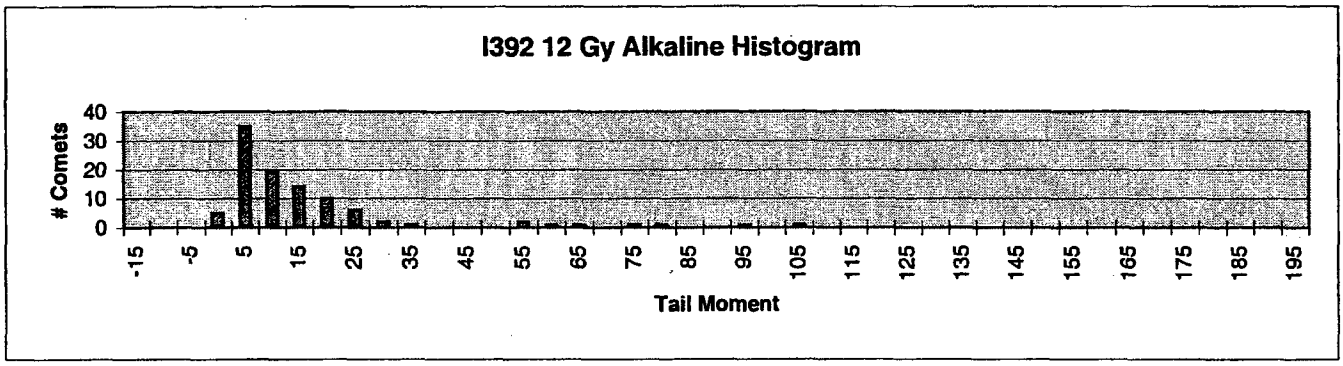

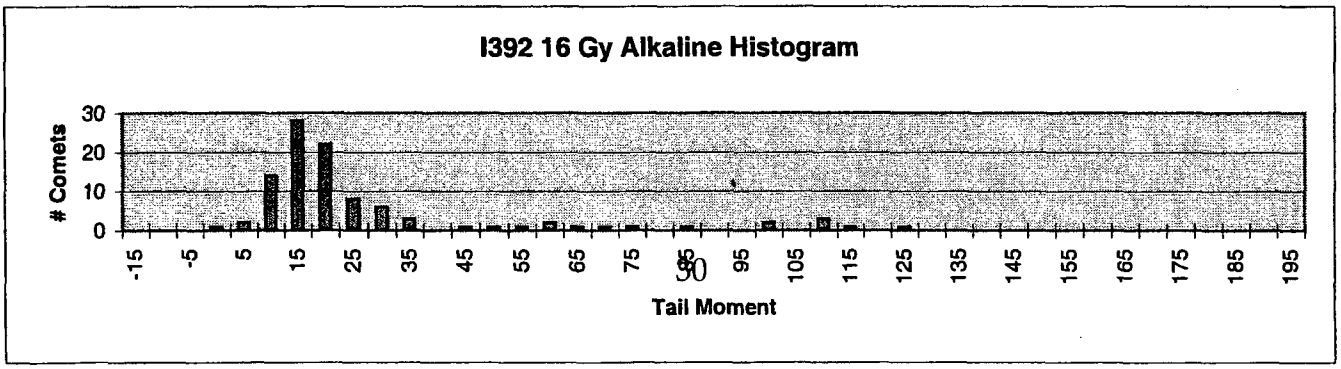

Figure 5: I401 Alkaline Comet Assay Tail Moment Histograms

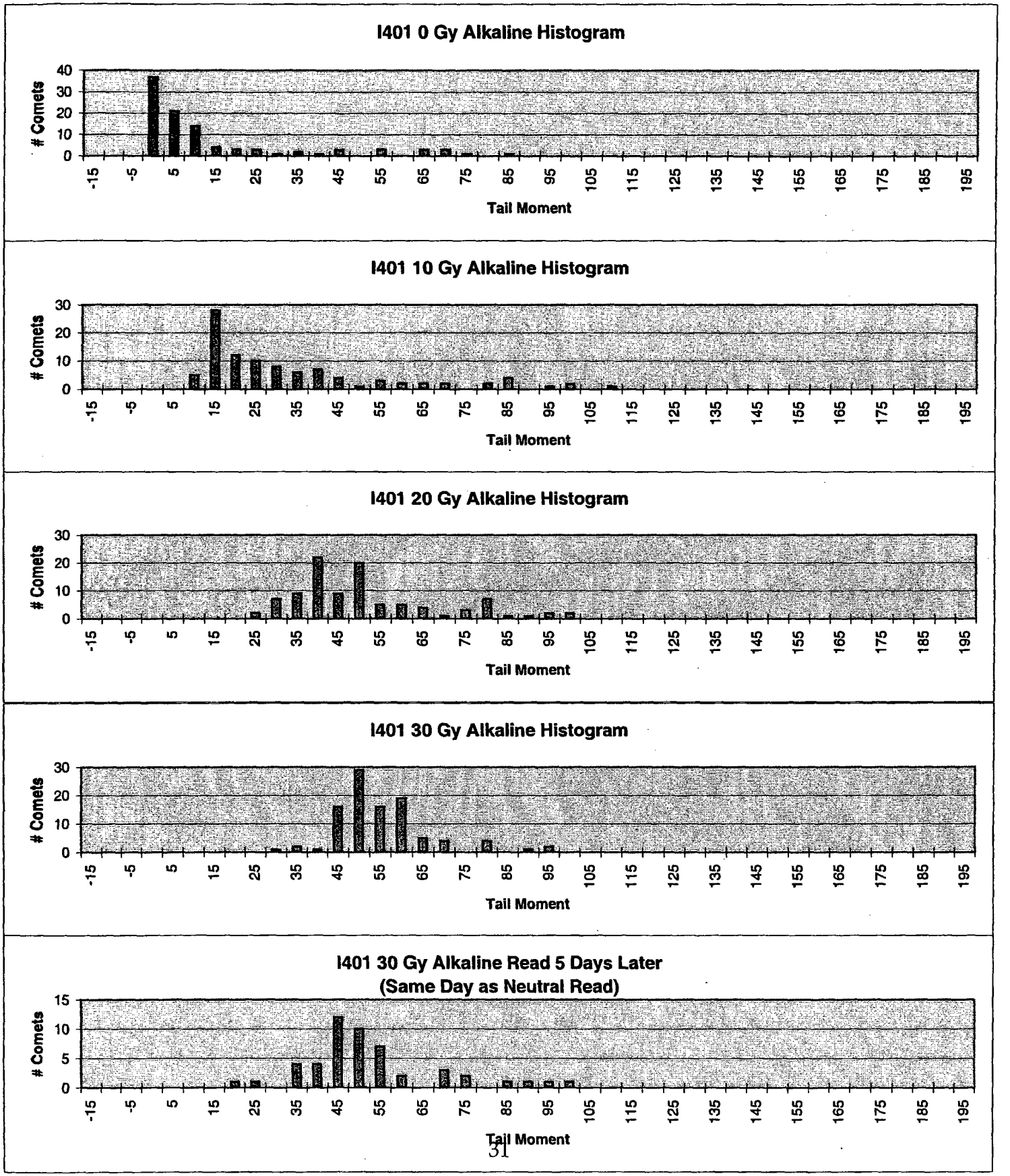

The 30 Gy slide was read five days after it was originally read to determine how time affects the tail moments. After five days, the histogram did not shift significantly.

Figure 6: I401 Alkaline and Neutral Comet Assay Median Tail Moment Trends

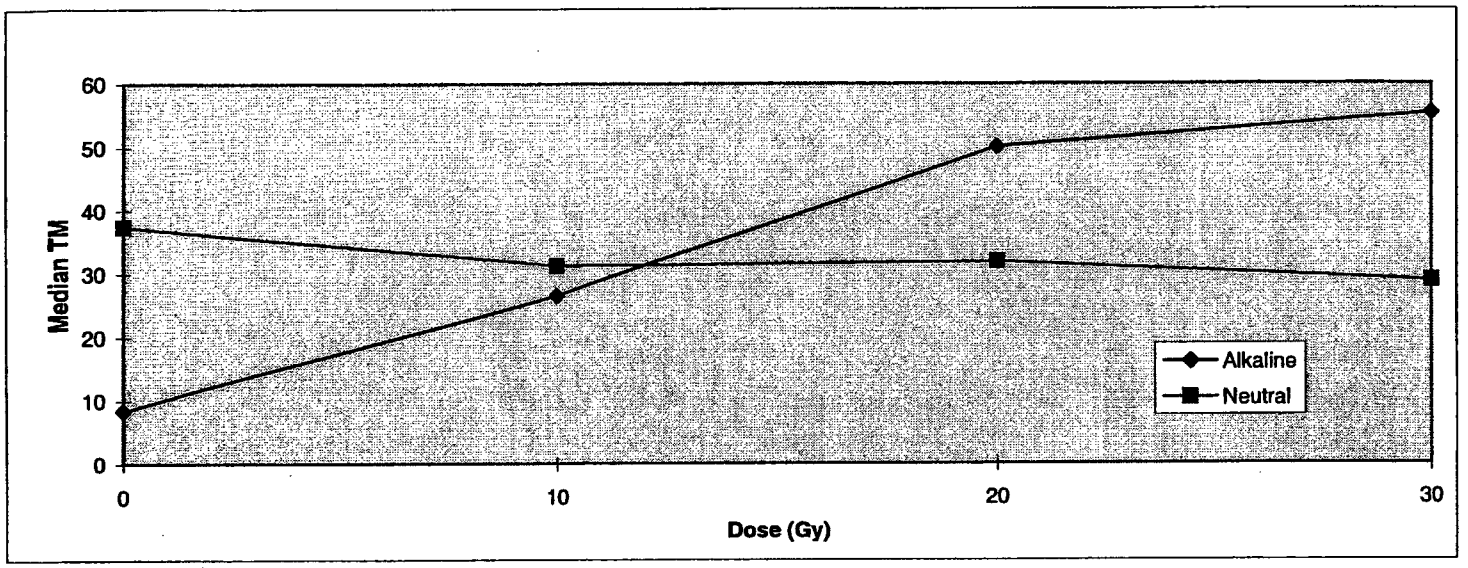

Figure 7: I401 Neutral Comet Assay Tail Moment Histograms

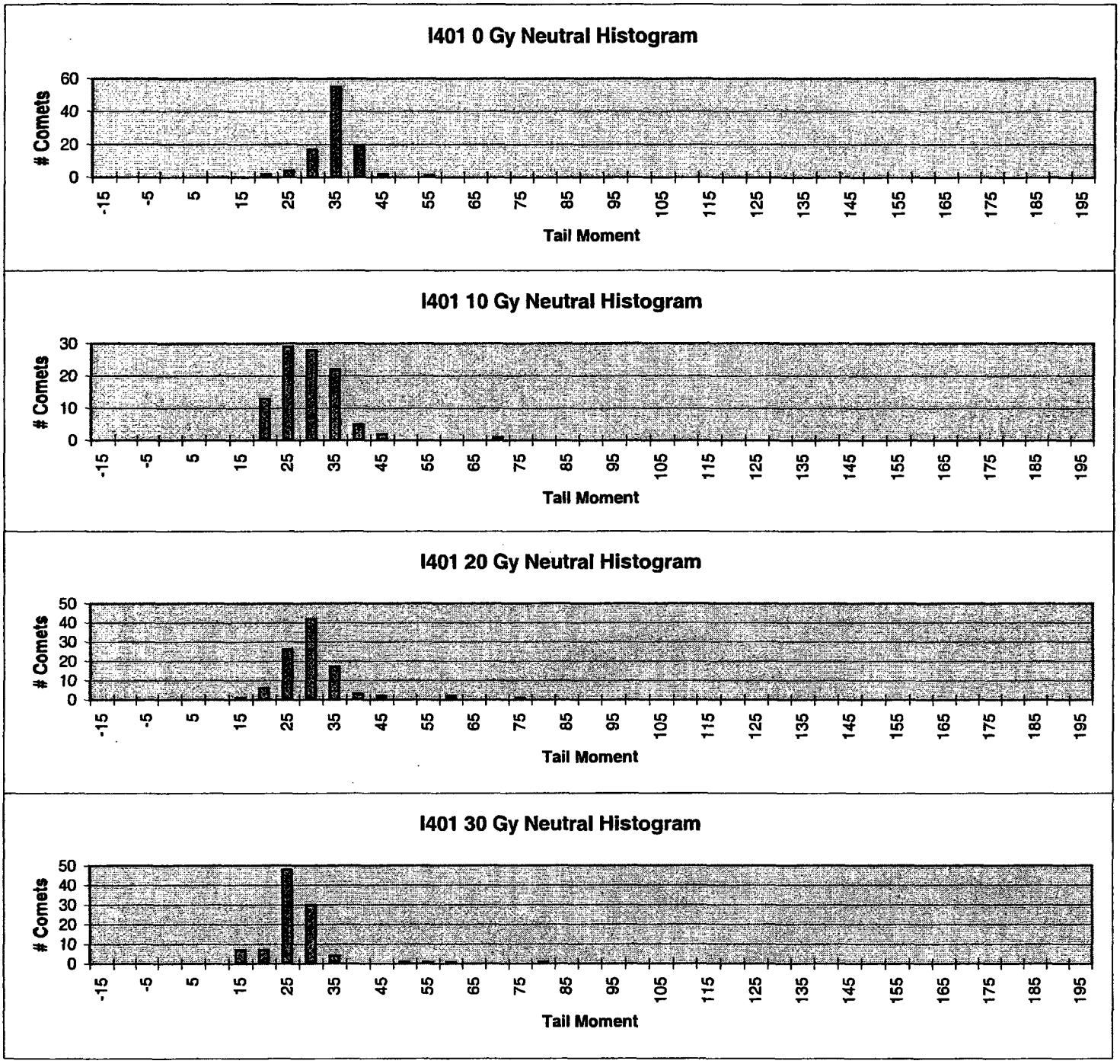

Figure 8: I438 Alkaline Comet Assay Tail Moment Histograms

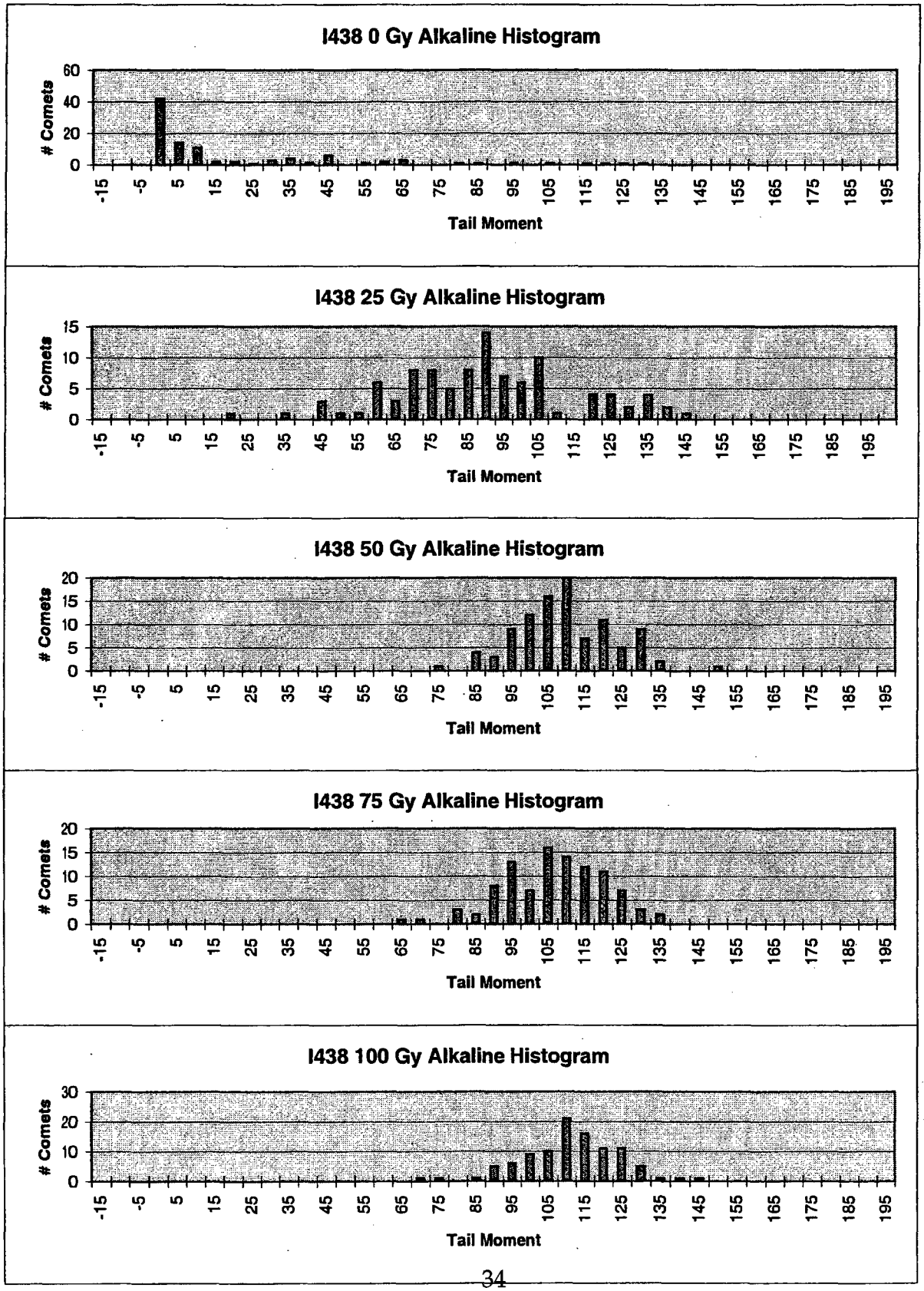

Figure 9: I438 Neutral Comet Assay Tail Moment Histograms

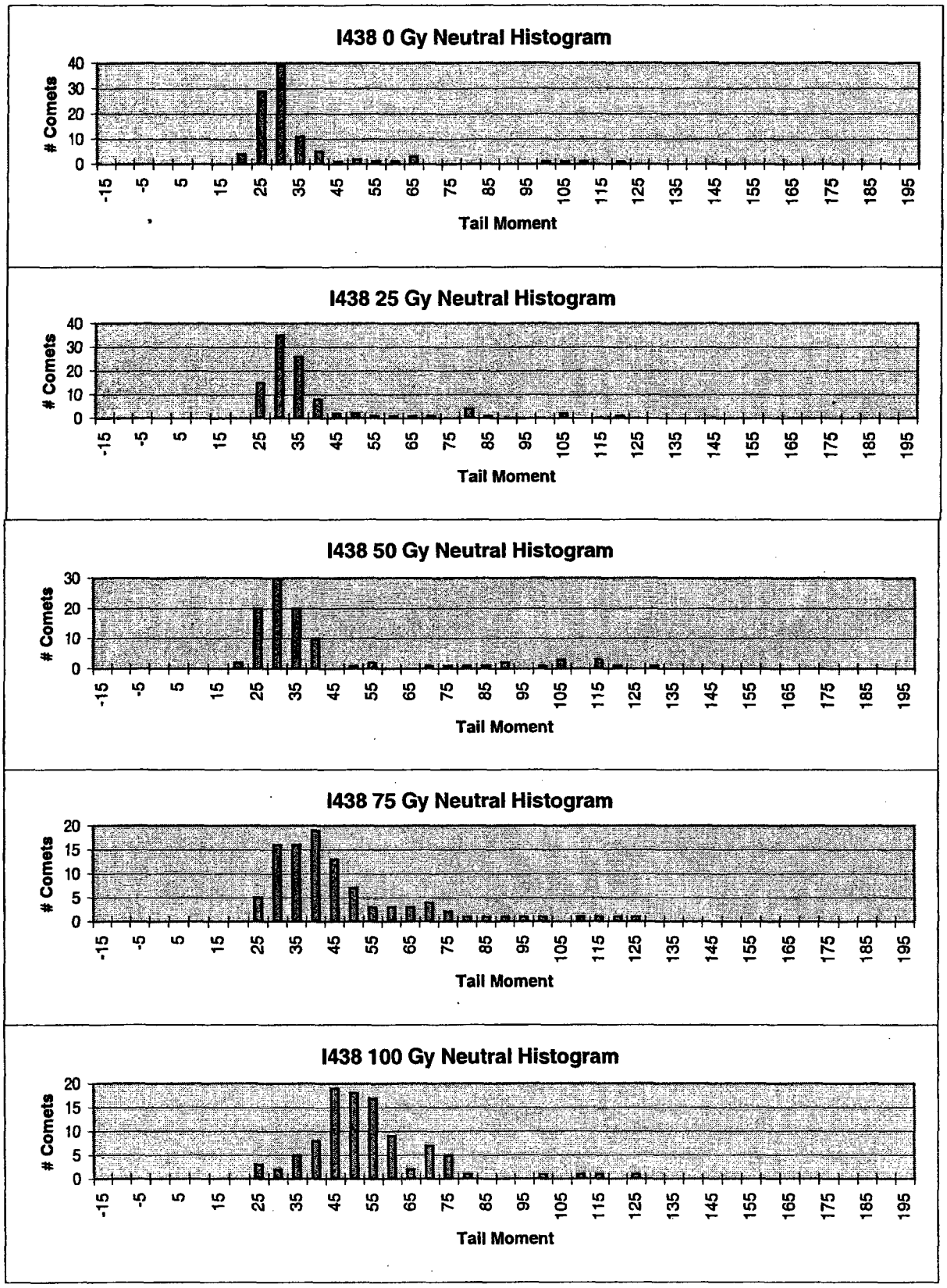

Figure 10: I438 and I444 Median Tail Moment Trends

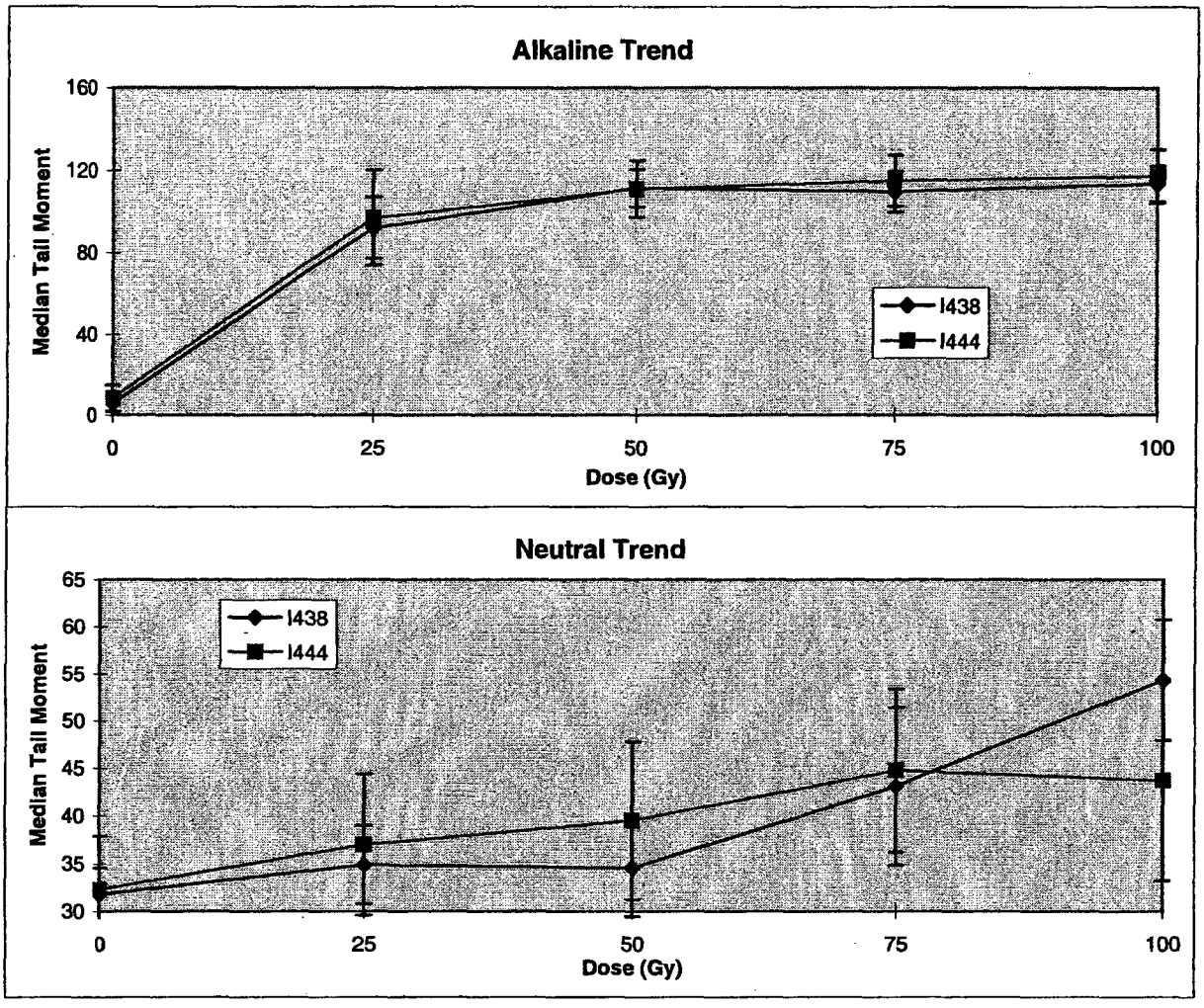

The alkaline comet assay median tail moment curves almost overlap, and within the error margins are essentially the same.

The neutral comet assay median tail moment trends are similar, but do not agree as well as the alkaline comet assay median tail moments do.

Figure 11: Scheme from Experiment I446

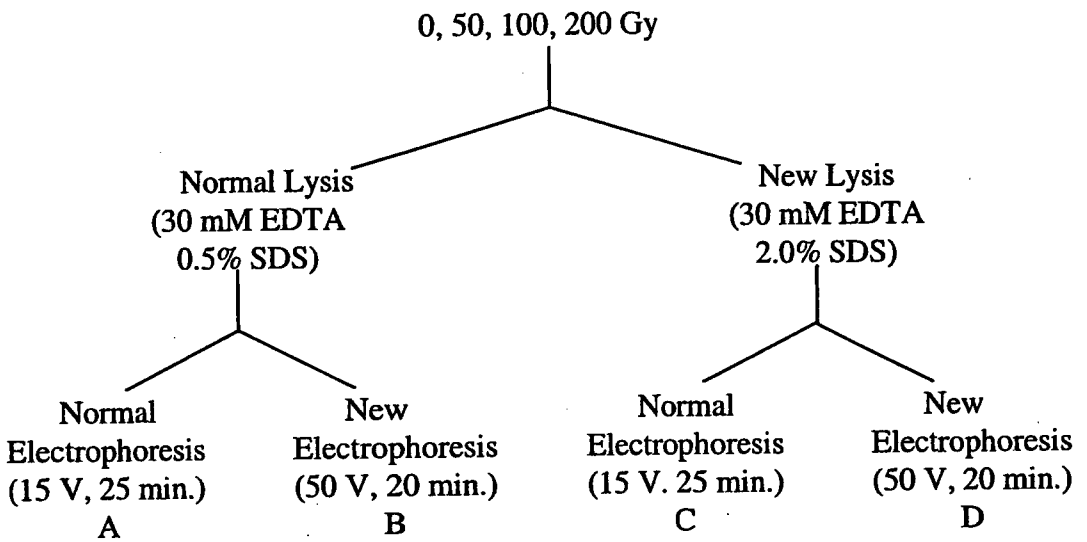

Figure 12: I446 Neutral Comet Assay Median Tail Moments with Treatment

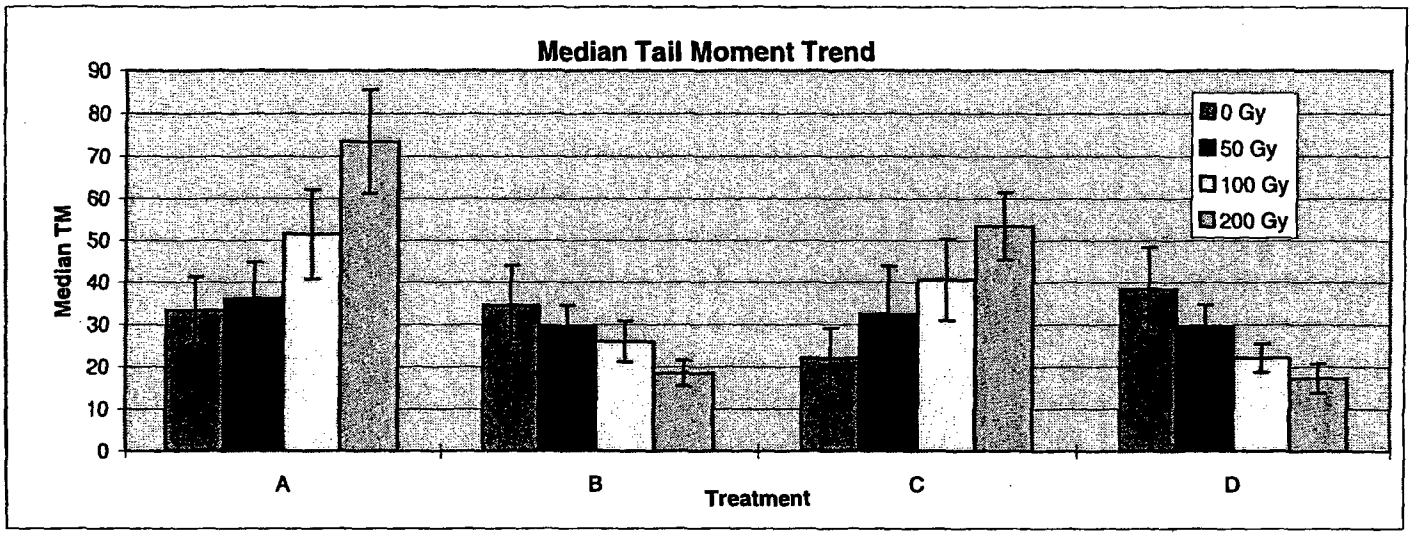

Details about the treatment conditions are in Figure 11. The best set of conditions is Condition C. Although the highest doses are better differentiated by Condition A, the more relevant lower doses are better differentiated by Condtion C. This was the result of a higher detergent concentration in the lysis buffer, which resulted in more complete lysis of the cells.

Figure 13: Scheme from Experiment I557

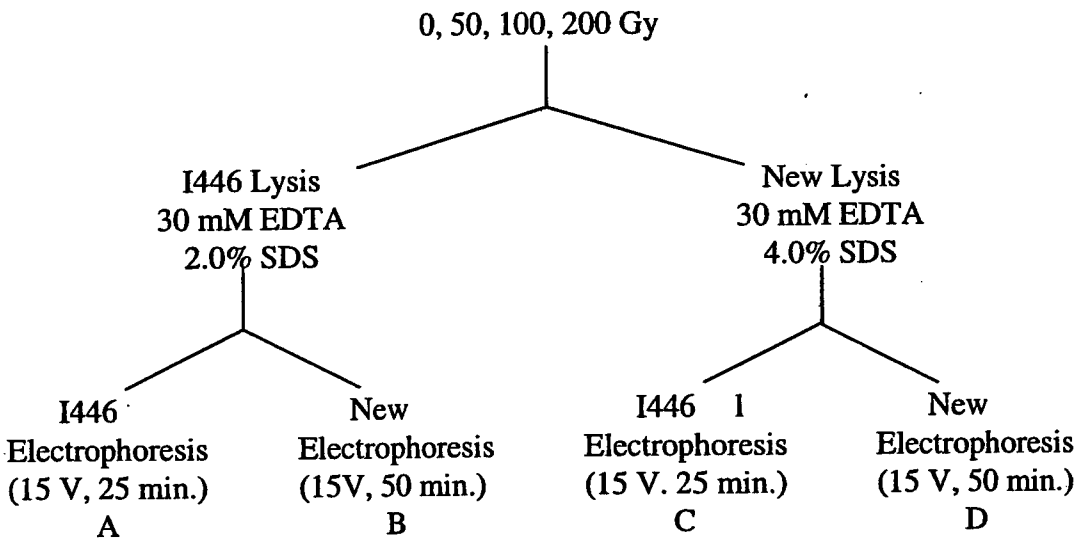

Figure 14: I557 Neutral Comet Assay Optimization of Conditions

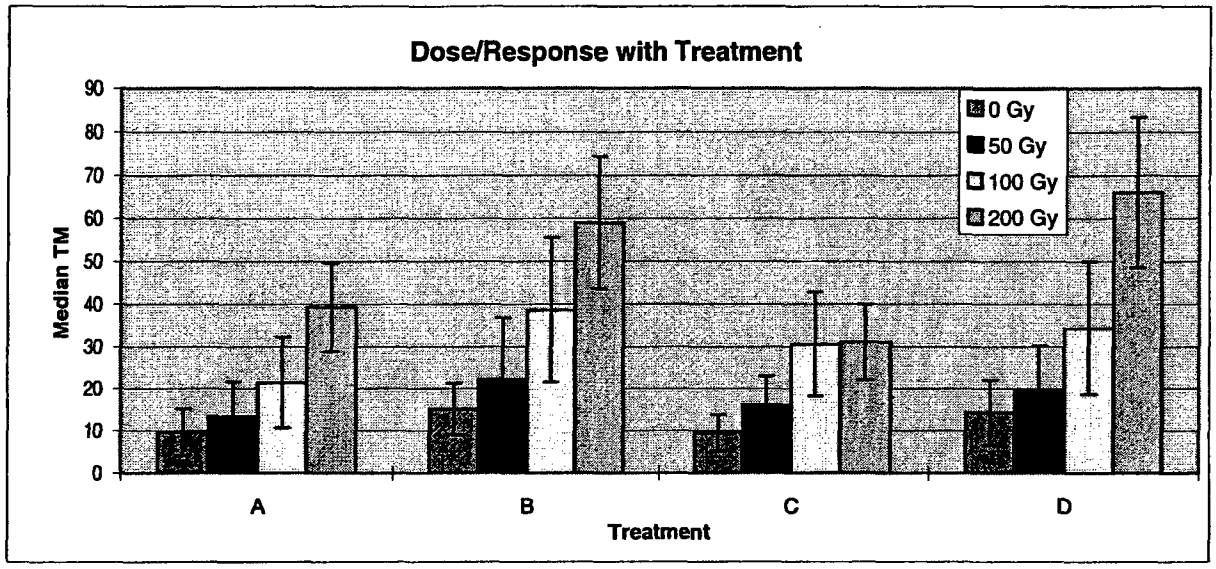

The conditions are detailed in Figure 13. Although the error bars still overlap, the conditions are improving the sensitivity of the assay. Further optimization of the system would only be specific to V79 cells, which are not the ultimate subject of the assay. No further optimization of the neutral conditions for V79 cells was performed.

Figure 15: I1015 Initial Alkaline Comet Assay Performed on Primary Rat Mammary Epithelial Cells

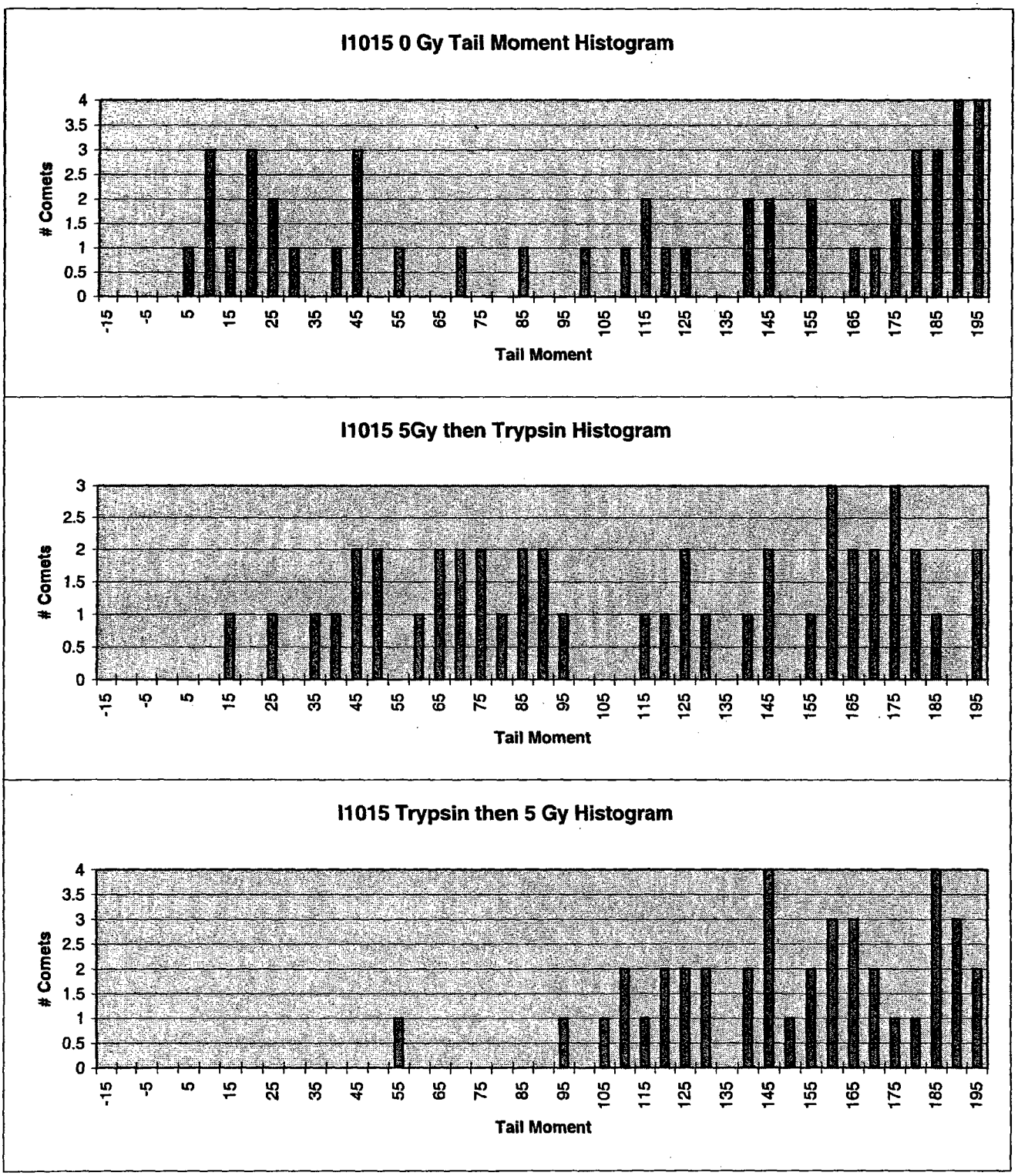

These histograms reveal that there is considerable background damage and that further optimization of the conditions is necessary.

Table 1: Conditions for K16, Alkaline Comet Assay on Primary Rat Mammary Epithelial Cells

Lysis Temperature:	4° C	25°C	4° C	25°C
Unwinding Temperature:	25°C	4° C	25°C	4° C
0 Gy	Slide 1	Slide 2	Slide 3	Slide 4
2.5 Gy	Slide 5	Slide 6	Slide 7	Slide 8
5 Gy	Slide 9	Slide 10	Slide 11	Slide 12
10 Gy	Slide 13	Slide 14	Slide 15	Slide 16

4°C indicates that the procedure was performed in the cold room.
25° indicates that the procedure was performed at room temperature.

Figure 16: K16 Alkaline Comet Assay with Primary Rat Mammary Epithelial Cells

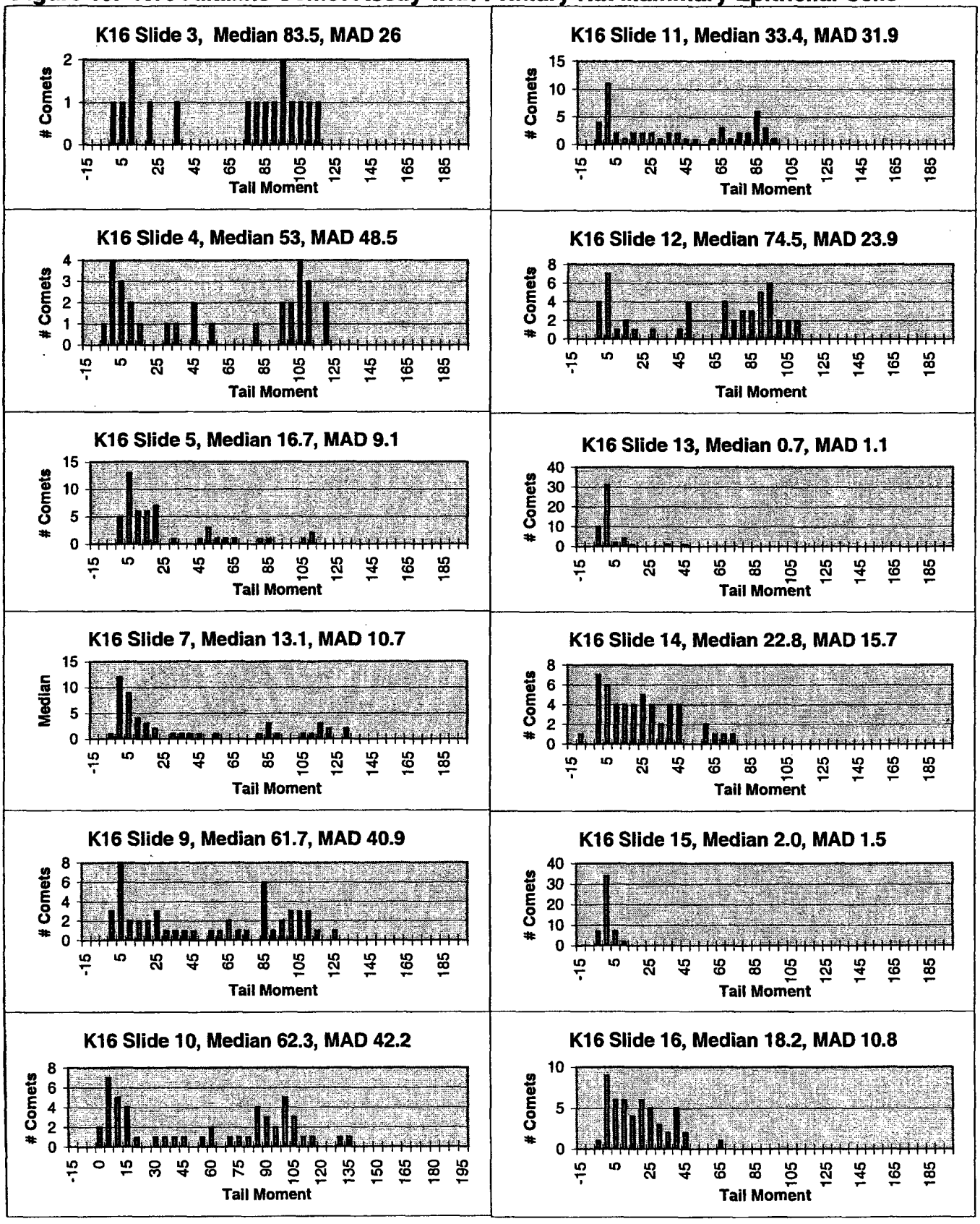

Conditions are detailed in Table 1. Graphs were produced for all conditions for which it was possible. In a number of slides, not enough comets were visible to analyze the slide.

Figure 17: Scheme from Experiment K25

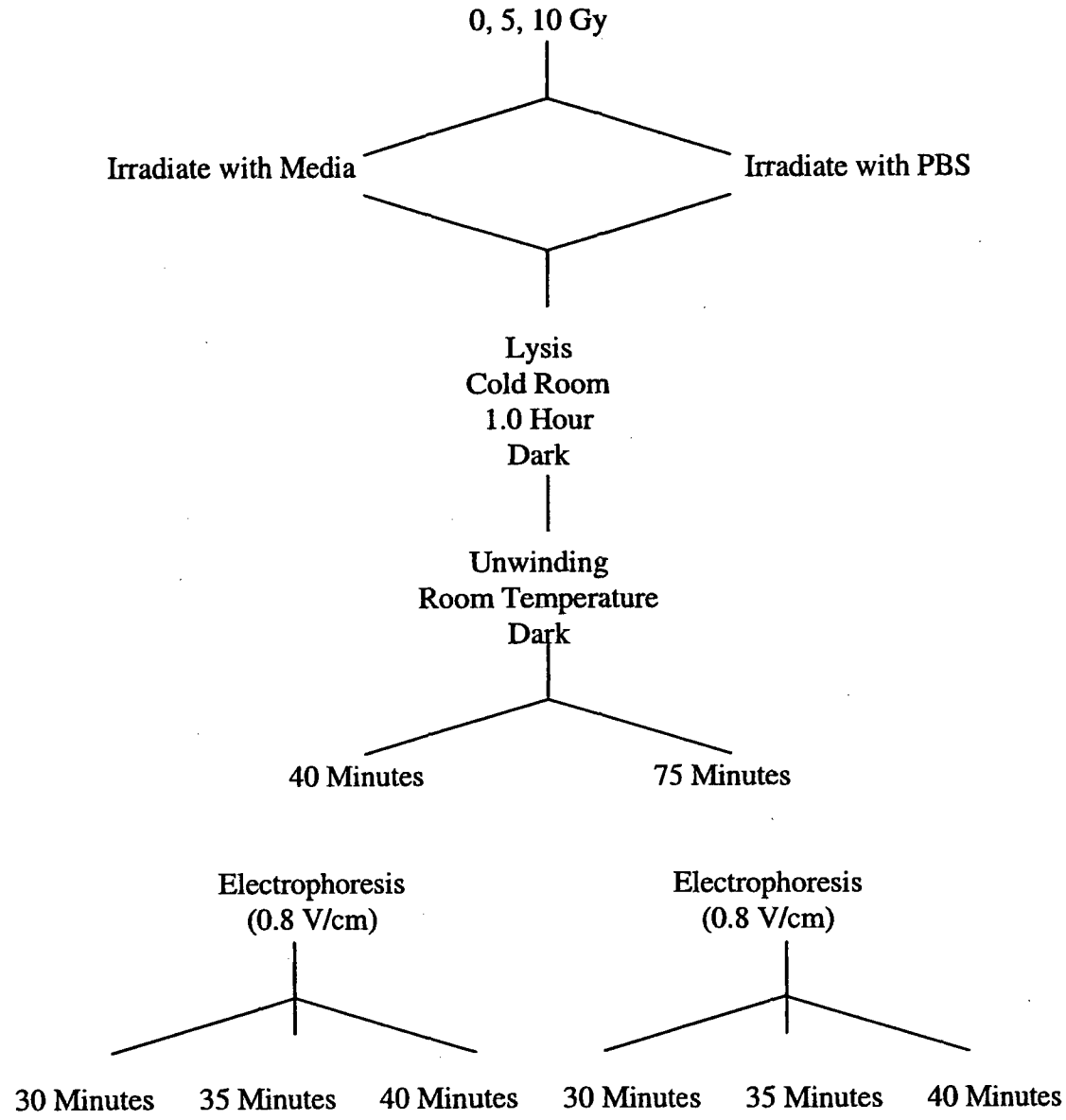

Figure 18: K25 Alkalkine Comet Assay on Primary Rat Mammary Epithelial Cells Condition Optimization

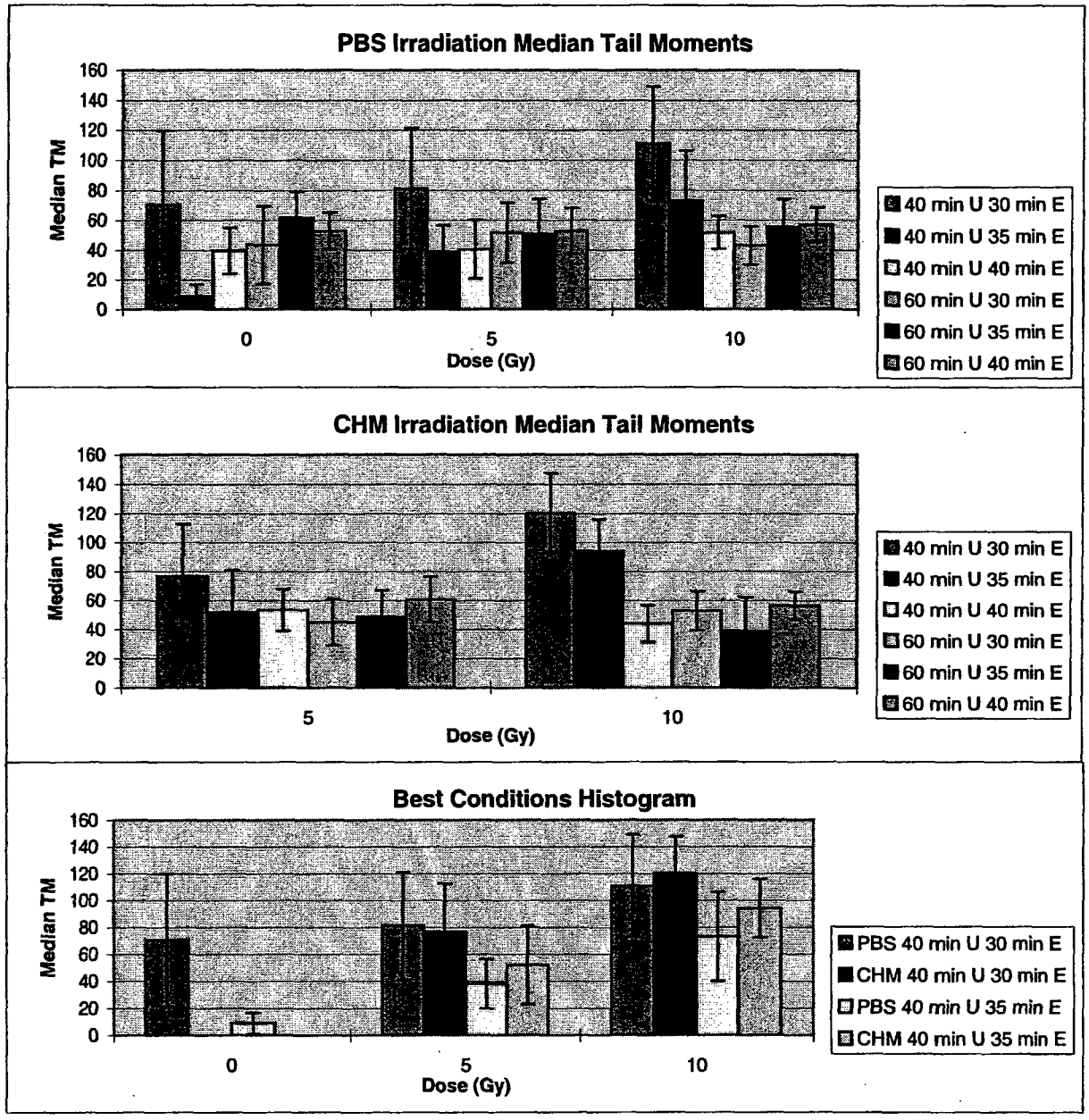

U stands for unwinding time, and E stands for electrophoresis time. The conditions which provided the best dose-response are plotted in the bottom graph. Although there is visible improvement from the last experiment, further optimization is still necessary.

Figure 19: Scheme from Experiment K47

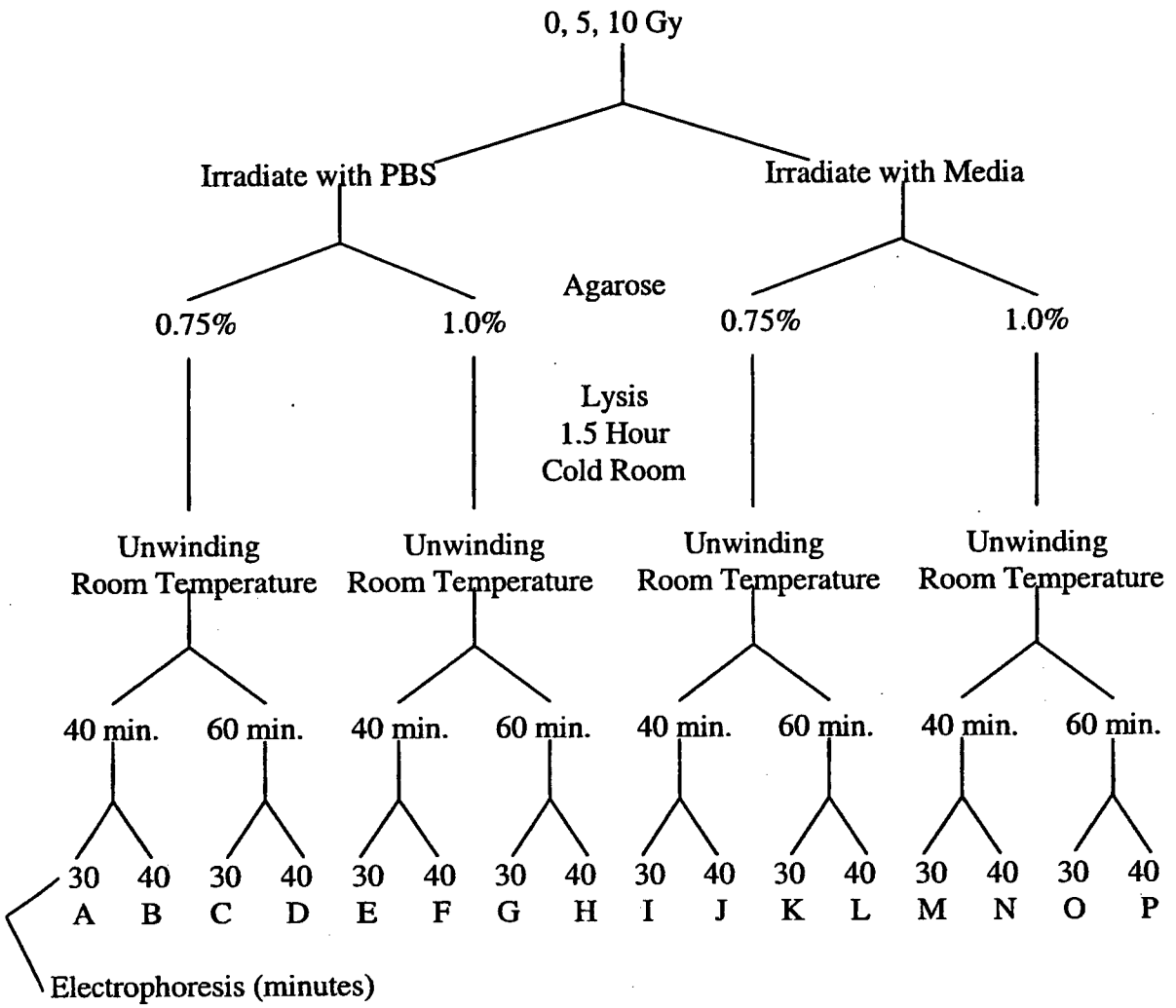

Figure 20: Alkaline Comet Assay on Primary Rat Mammary Epithelial Cells with Improved Trypsinization

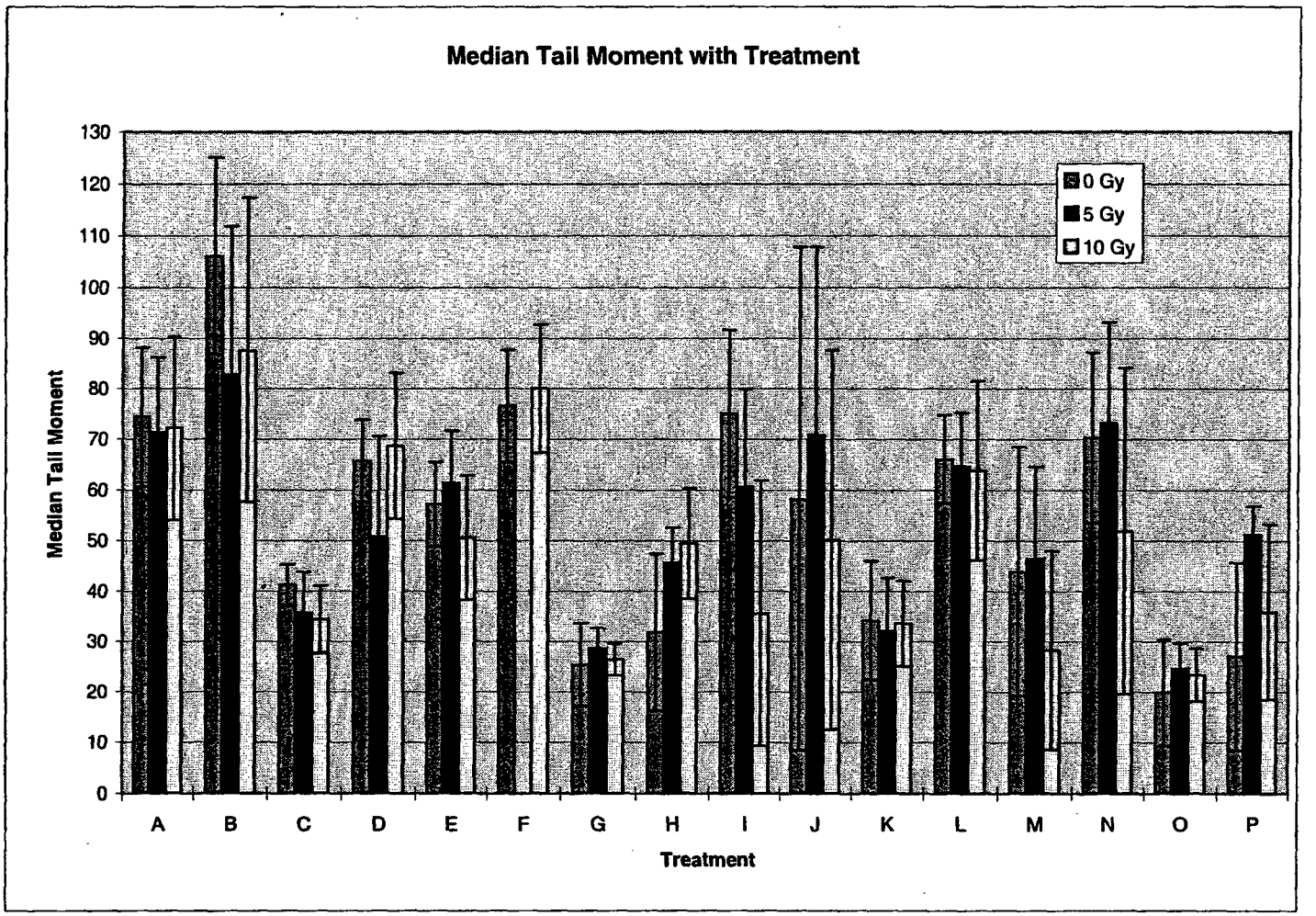

Treatment conditions are detailed in Figure 19. The best conditions were determined to be those with the best separation of median tail moments between 0 and 5 Gy. See the text for a discussion of the 10 Gy values. Conditions H and P (1% agarose, room temperature unwinding for 60 minutes, 40 minute electrophoresis) appeared to be the best.

Figure 21: K47 Histograms from the Best Conditions for the Alkaline Comet Assay for Primary Rat Mammary Epithelial Cells

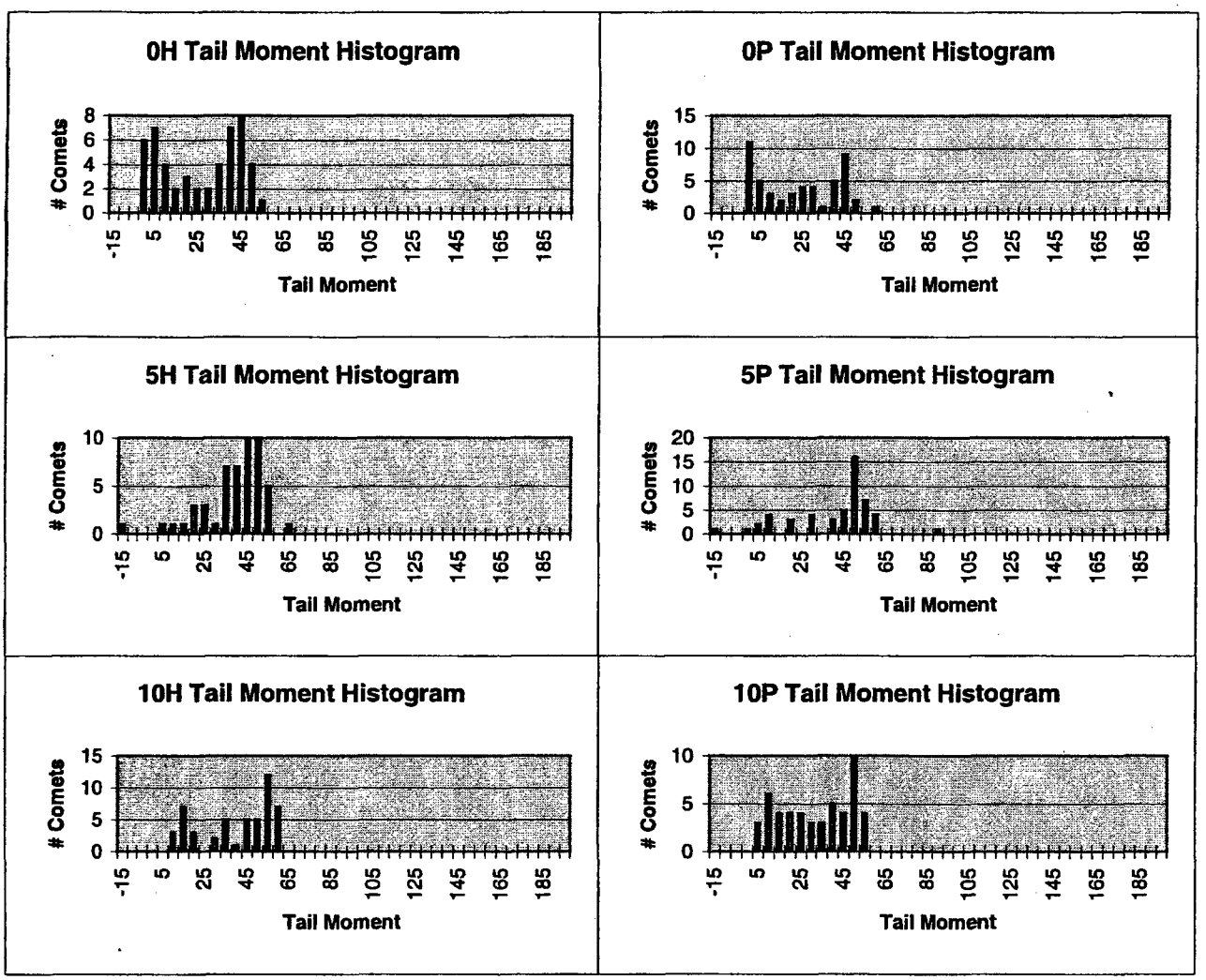

The conditions used on these slides are as follows: 1% agarose, 60 minutes unwinding at room temperature, followed by a 40 minute electrophoresis. The only difference was that the slides designated as H were irradiated with PBS on them, while those designated as P were irradiated with complete hormonal medium on them. These histograms still are not ideal, but further optimization should produce workable conditions.

Aim 5: Is the lack of TGFα production by cells of the immature mammary gland related to increased sensitivity to radiation induced cell killing?

The purpose of this aim is to determine if the absence of transforming growth factor α (TGFα) in the immature mammary gland plays a role in the increased sensitivity to ionizing radiation as compared to that of the mature gland. This aim is predicated on the assumption that the immature mammary gland does not produce TGFα, while the mature gland does. The basis for this assumption is a publication reporting that TGFα mRNA was not detected in the immature mouse mammary gland, but it was in the mature gland.

The assumption that the immature rat mammary gland does not produce TGFα was based on a study of murine mammary glands. However, other more recent studies on the rat mammary gland contradict this assumption. First, the failure to detect TGFα mRNA may not indicate the absence of TGFα protein, since Smith, *et al.* could not detect TGFα mRNA in RNA isolated from lactating rat mammary gland, where TGFα activity was found (1989). Also, McAndrew *et al.*(1994) report that the level of TGFα mRNA doesn't necessarily directly relate to the amount of protein, since they found a decrease in immunoreactive TGFα in the pregnant rat mammary gland, but others reported an increase in TGFα mRNA expression at that stage (Liscia *et al.* 1990 and Snedeker *et al.* 1991). McAndrew *et al.* reported no difference in the immunolocalization of TGFα in the mammary glands of immature (21 day old) and mature (50 day old, the oldest rats studied) female Ludwig Wistar OLA rats (1994). The 50 kDa immunoreactive TGFα was found in both the growing terminal end buds and alveolar buds, with the most staining found in the myoepithelial cells. In fact, the epithelial ductal cells of 1- and 6-day old rats stained more strongly for TGFα than the epithelial cells of the older rats, although the myoepithelial staining was stronger in the 21-day and 50-day old rats.

On one hand, the murine gland appears to age-differentially express TGFα mRNA. On the other hand, the Ludwig Wistar OLA 21- and 50- day old rats express the same amount of protein. However, the rats used in the present study will be Fischer 344 rats, which might differ from the Ludwig Wistar OLA rat. This discrepancy must be reconciled before serious work can begin on this aim.

Toward that end, a TGFα immunohistochemistry system kit has been purchased, and optimal primary antibody concentrations have been determined for staining both immature and mature rat mammary glands. Mammary glands from mature and immature irradiated (because the slides are available) and control rats will be analyzed by immunohistochemistry for TGFα. If age-differential staining is observed, then work will continue with this aim. If not, a logical candidate gene identified in Aim 6 will be further studied under Aim 5.

References

Liscia, D.S., Merlo, G., Ciardiello, R., Kim, N., Smith, G.H., Callahan, R., and Salomon, D.S. Transforming growth factor-alpha messenger RNA localization in the developing adult rat and human mammary gland by *in-situ* hybridization. *Developmental Biology* 140: 123-31, 1990.

McAndrew, J., Rudland, P.S., Platt-Higgins, A.M., and Smith, J.A. Immunolocalization of alpha-transforming growth factor in the developing rat mammary gland *in vivo*, rat mammary cells *in vitro* and in human breast diseases. *Histochemical Journal* 26: 355-366, 1994.

Smith, J.A., Barraclough, R., Fernig, D.G., and Rudland, P.S. Identification of alpha transforming growth factor as a possible local trophic agent for the mammary gland. *Journal of Cellular Physiology* 141: 362-370, 1989.

Snedeker, S.M., Brown, C.F., and DiAugustine, P. Expression and functional properties of transforming growth factor α and epidermal growth factor during mouse mammary gland ductal morphogenesis. *Proceedings of the National Academy of Sciences, USA* 88: 276-280, 1991.

Aim 6: How is the spectrum of gene expression in the immature and mature mammary glands different with regard to genes which could directly or indirectly confer altered DNA repair capacity?

Subtraction cloning genes differentially expressed in mammary glands from 3-wk and 8-wk old F344 rats

Gene expression regulation plays an essential role in the animal developmental process and the associated biological response to exogenous stimuli. Rat mammary epithelial cells of different ages demonstrate different sensitivity to radiation-induced cell killing. Previous studies have suggested that age-related radiation sensitivity is attributed to the epithelial cells themselves rather than the environment in which they reside. The gene expression pattern of a given tissue in an animal may vary through different developmental stages. The observed variation in radiation sensitivity of mammary epithelial cells from different age groups may reflect the different gene expression patterns of corresponding developmental stages. The purpose of this study is to investigate the different gene expression spectra in the immature and mature mammary gland, and identify genes which could directly or indirectly confer an altered cellular recovery capacity following cytotoxic and genotoxic, such as radiation-induced, damage.

Materials and methods

Animals

Virus-free F344 female and male rats were obtained from Harlan Sprague-Dawley, Inc. (Indianapolis, IN). The breeding of the rats to create 3 week old F344 female rats was performed at our facility. 8 week old F344 female rats were obtained directly from Sprague-Dawley, Inc. All rats were provided with Teklad Lab Blox (Harlan Teklad, Madison, WI) and acidified water ad libitum. The rats were housed under a 12 hour light and 12 hour dark cycle.

RNA Isolation and cDNA Synthesis

Lower mammary glands (glands D, E and F) were collected from 3-week and 8-week olds female F344 rats and immediately frozen in liquid nitrogen. To isolate the total RNA, 200 mg frozen

tissue was homogenized in 4 ml RNAzol B reagent (Tel-Test) with a Polytron homogenizer at setting 8 for 30 seconds. The total RNA was extracted by following the manufacturer's protocol. Poly(A)+ RNA was then prepared from the total RNA using RNeasy kits (QIAGEN). Double-stranded cDNA (ds cDNA) was synthesized from poly(A)+ RNA using the SuperScript Choice System (Life Technologies). Tester and driver ds cDNAs were prepared from the two mRNA samples under comparison.

Subtraction cloning of differentially expressed sequences

The differentially expressed sequences in 3-week and 8-week old rat cDNAs were screened using the PCR-Select cDNA subtraction kit (CLONTECH Laboratory, Inc.) as shown in Figure 1. To maximize the subtraction process, the tester and driver cDNAs were separately digested with *Rsa*I to obtain shorter, blunt-ended fragments. When the 3-wk sample was used as the tester cDNA, the 8-wk sample was the driver cDNA and *vice versa*. For each sample, two tester populations were created with different adaptors, but the driver cDNA had no adaptors. During the first hybridization, two tester cDNA populations were separately hybridized to driver cDNA to enrich those differentially expressed sequences. The two hybridizations were then mixed together during the second hybridization to generate PCR templates of those differentially expressed sequences. Two rounds of PCR amplification was performed to normalize and enrich those differentially expressed sequences. The subtraction screening was carried out following the manufacturer's protocol with some modification. During the second round of PCR, subpopulation nested PCR primers (Table I, pg.) were used to replace the nested PCR primer 2R. The conditions for primary PCR are 75°C for 5 min, followed by 27 cycles of 94°C for 45 sec, 66°C for 30 sec and 72°C for 1.5 min. The conditions for secondary PCR are 19 to 23 cycles of 94°C for 45 sec, 68°C for 30 sec and 72°C for 1.5 min. The secondary PCR products from subtracted 3-wk and 8-wk F344 mammary gland cDNAs were separated on 5% polyacrylamide gels and visualized by Fluoroimager (Molecular Dynamics) after staining with SYBR Gold nucleic acid gel stain (Molecular Probes).

Subcloning and Characterizing the subtracted cDNA sequences

The entire PCR product mixture of each primer set was subcloned into the pCRII vector using the TA cloning kit (InVitrogen). Colonies with inserts were identified by PCR with primers flanking the cloning sites. Clones with inserts were sequenced and/or examined for differential expression between 3-wk and 8-wk F344 mammary glands by reverse northern dot blotting. Clones with different signal levels identified by dot blot were further examined by ribonuclease protection assay (RPA) using a RPAII kit (Ambion).

Results and Discussion

Different patterns were observed between PCR-amplified subtracted 3-wk and 8-wk cDNAs (Fig. 2). PCR products of 8-wk subtracted cDNAs were subcloned into the pCRII plasmid vector, and approximately 300 clones were obtained. Among those subclones, 96 clones were examined by reverse northern dot blot. Several clones have demonstrated differential expression between 3-wk and 8-wk mammary glands (Fig. 3). Sequence analysis revealed three of them as rat lipopolysaccharide binding protein (LBP), α-casein and κ-casein cDNA, respectively. Casein genes are markers for mammary differentiation (1, 2). Their expression in rat mammary glands is known to be associated with sexual maturation. The isolation of α-casein and κ-casein cDNA confirmed the previous observation and the success of the PCR-select subtraction procedure. The differential expression of LBP mRNA was further confirmed by RPA. It is expressed only in

8-wk mammary gland (Fig. 4). It has been suggested that LPB plays a role in host immune responses to injury and infection, however, the mechanism remains to be characterized (3). The remaining putative clones of differentially expressed sequences showed little homology to GenBank database. These clones need to be verified by RPA or other quantitative analysis before further characterization.

More than half of the clones examined by reverse northern dot blot were under the detection sensitivity, which indicated that they represented sequences in low abundance. Direct sequencing of these clones would provide some clue to their identities and facilitate further characterization. Less than 10% of the clones examined by dot blot represented those highly abundant sequences with equivalent levels in both 3-wk and 8-wk population. This indicated that the subtraction process was efficient in removing most of the abundant sequences present in both tester and driver cDNA. Those abundant sequences that escaped the subtraction process were good references for signal normalization in the reverse northern dot blot.

An alternative method to identify differentially expressed sequences is to subclone them from the polyacrylamide gel. The secondary PCR products of subtracted cDNA resolved on a polyacrylamide gel can be visualized by silver staining (4) and excised from the gel. Each band or bands can be PCR-reamplified and subcloned for further characterization. Such studies are now underway.

Conclusions

Multiple differentially expressed sequences were isolated from a subtracted 8-wk F344 cDNA library by a PCR-select subtraction method. This indicated that the subtraction procedure is successful in isolating differentially expressed sequences present in two populations. Two out of three cDNA clones characterized encode the milk proteins α-casein and κ-casein, suggesting that more clones isolated in this study will be physiologically relevant to the maturation of the mammary gland. The remaining 200 plus clones are currently under investigation. This study will provide a handful of markers for the molecular anatomy of the developing mammary gland. In addition, we may also identify, among those differentially expressed sequences, the ones that directly or indirectly confer altered cellular recovery capacity following radiation-induced damage.

REFERENCES

1. Topper, Y.J. and Freeman, C.S. Multiple hormone interaction in the developmental biology of the mammary gland. Physiol. Rev., 60:1049-1106, 1980.
2. Rosen, J.M. Milk protein gene structure and expression. In: M.C. Neville, and C.W. Daniel (eds), The Mammary Gland: Development, Regulation, and Function, pp. 301-322. New York: Plenum Press, 1987.
3. Grace L. Su, Paul D. Freeswick, David A. Geller, Qi Wang, Richard A. Shapiro, Yong-Hong Wan, Timothy R. Billiar, David J, Tweardy, Richard L Simmons, and Stewart C, Wang. Molecular Cloning, Characterization, and Tissue Distribution of Rat Lipopolysaccharide Binding Protein. J. of Immunology 153: 743-752, 1994.
4. Sanguinetti, C.J., Dias Neto, E., and Simpson, A.J. Rapid silver staining and recovery of PCR products separated on polyacrylamide gels. Biotechniques 17(5), 914-921, 1994.

Table I. Subpopulation primers for the second PCR

Subpopulation primer	Sequence*
Nested PCR primer 2R/A	AGCGTGGTCGCGGCCGAGGTA
Nested PCR primer 2R/C	AGCGTGGTCGCGGCCGAGGTC
Nested PCR primer 2R/G	AGCGTGGTCGCGGCCGAGGTG
Nested PCR primer 2R/T	AGCGTGGTCGCGGCCGAGGTT
Nested PCR primer 2R/ACA	AGCGTGGTCGCGGCCGAGGTACA
Nested PCR primer 2R/ACC	AGCGTGGTCGCGGCCGAGGTACC
Nested PCR primer 2R/ACG	AGCGTGGTCGCGGCCGAGGTACG
Nested PCR primer 2R/ACT	AGCGTGGTCGCGGCCGAGGTACT

* subpopulation Nested PCR primer 2R/ differs from primer 2R by containing additional nucleotide(s) variant at 3' end.

Figure Legends

Fig.1 Schematic diagram of PCR-select cDNA subtraction. The cDNA in which specific transcripts are to be found is called "tester" and the reference is called "driver". Type **e** molecules are formed only if the sequence is up-regulated in the tester cDNA. Solid lines represent the RsaI-digested tester or driver cDNA. Solid boxes represent the outer part of the Adaptor 1 and 2R longer strands and corresponding PCR primer 1 sequence. Clear boxes represent the inner part of the Adaptor 1 and the corresponding Nested PCR primer 1 sequence; shaded boxes represent the inner part of Adaptor 2R and the corresponding Nested primer 2R sequence.

Fig. 2 Display of PCR-amplified subtractive library. The secondary PCR products of the subtracted mammary glands. Nested PCR primer 1 and Nested PCR subpopulation primer 2R/ (Table I) were used in the secondary PCR. The 3' end of each subpopulation primer 2R/ is indicated. Lanes 1 through 8, subtracted 3-wk cDNA samples; lanes 9 through 16, subtracted 8-wk cDNA samples.

Fig. 3 Reverse northern dot blot. The PCR-amplified inserts of ninety six clones were blotted to duplicate Hybond-N membranes. Each membrane was hybridized with the ^{32}P-labeled cDNA probe derived from the 3-wk and 8-wk F344 mammary gland mRNAs, respectively. The hybridized membranes were washed under high stringency conditions and exposed to a phosphoimager cassette. Clones with a signal ratio higher than 3 are highlighted by dashed circles. Three clones verified by cDNA sequencing are listed below: A8, lipopolysaccharide binding protein (LBP); B9, α-casein; D4, κ-casein.

Fig. 4 Ribonuclease protection assay of LBP mRNA in F344 mammary glands. Ten μg of 3-wk and 8-wk mammary gland total RNA were hybridized to ^{32}P-labeled LBP and 36B4 riboprobes and 42° C overnight. Additional reactions containing yeast tRNA added to each probe were used as controls. After RNase A1/H digestion, the protected probes were resolved on 6% denaturing polyacrylamide gels at 225 volts for 1 hour in TBE buffer. The gels were then dried onto 3MM chromatography paper and exposed to phosphoimager cassettes overnight and analyzed.

Figure 1

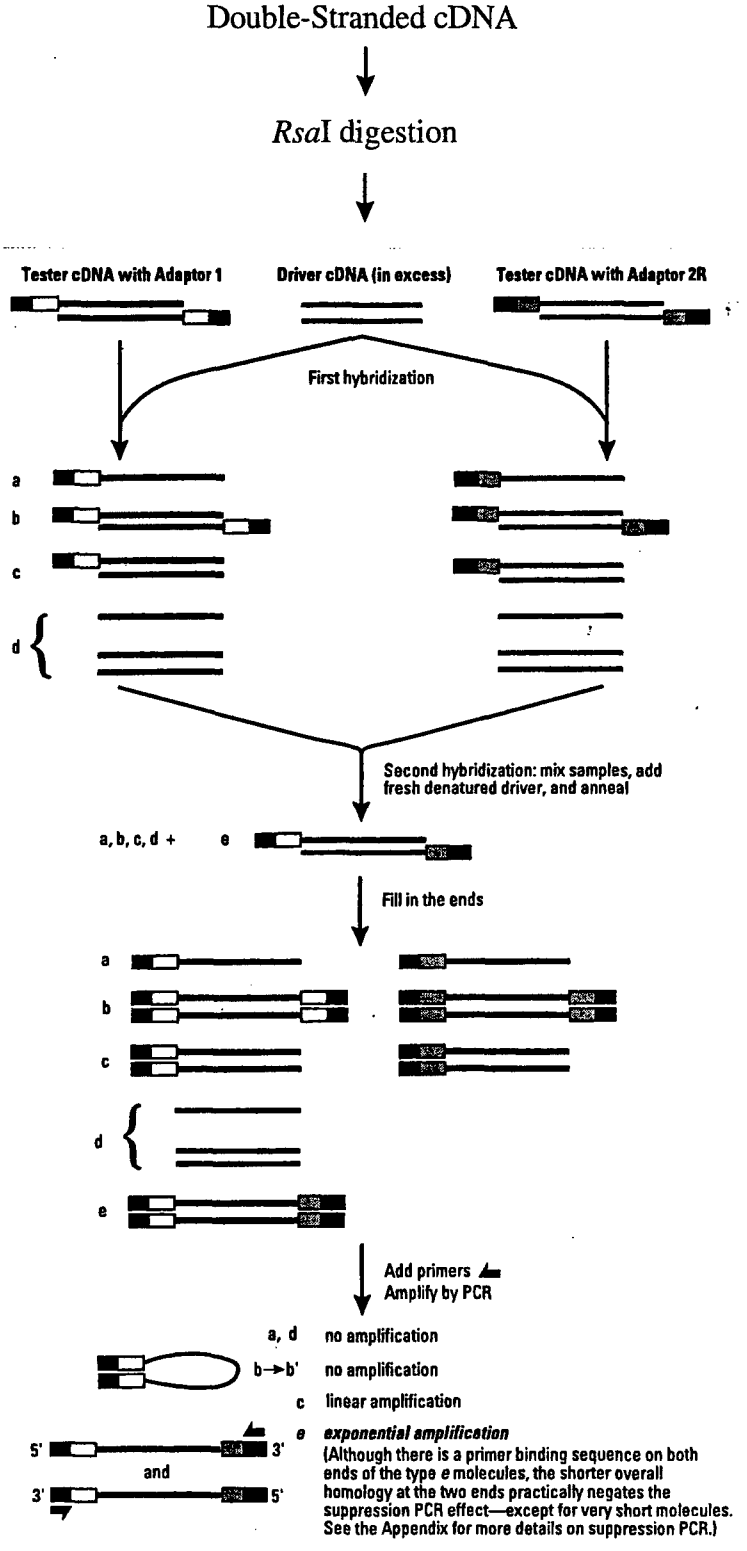
Double-Stranded cDNA
RsaI digestion
Tester cDNA with Adaptor 1
Driver cDNA (in excess)
Tester cDNA with Adaptor 2R
First hybridization
a
b
c
d
Second hybridization: mix samples, add fresh denatured driver, and anneal
a, b, c, d +
e
Fill in the ends
a
b
c
d
e
Add primers
Amplify by PCR
a, d
no amplification
b→b'
no amplification
c
linear amplification
e
exponential amplification
(Although there is a primer binding sequence on both ends of the type e molecules, the shorter overall homology at the two ends practically negates the suppression PCR effect—except for very short molecules. See the Appendix for more details on suppression PCR.)
5'
3'
and
3'
5'

Figure 2

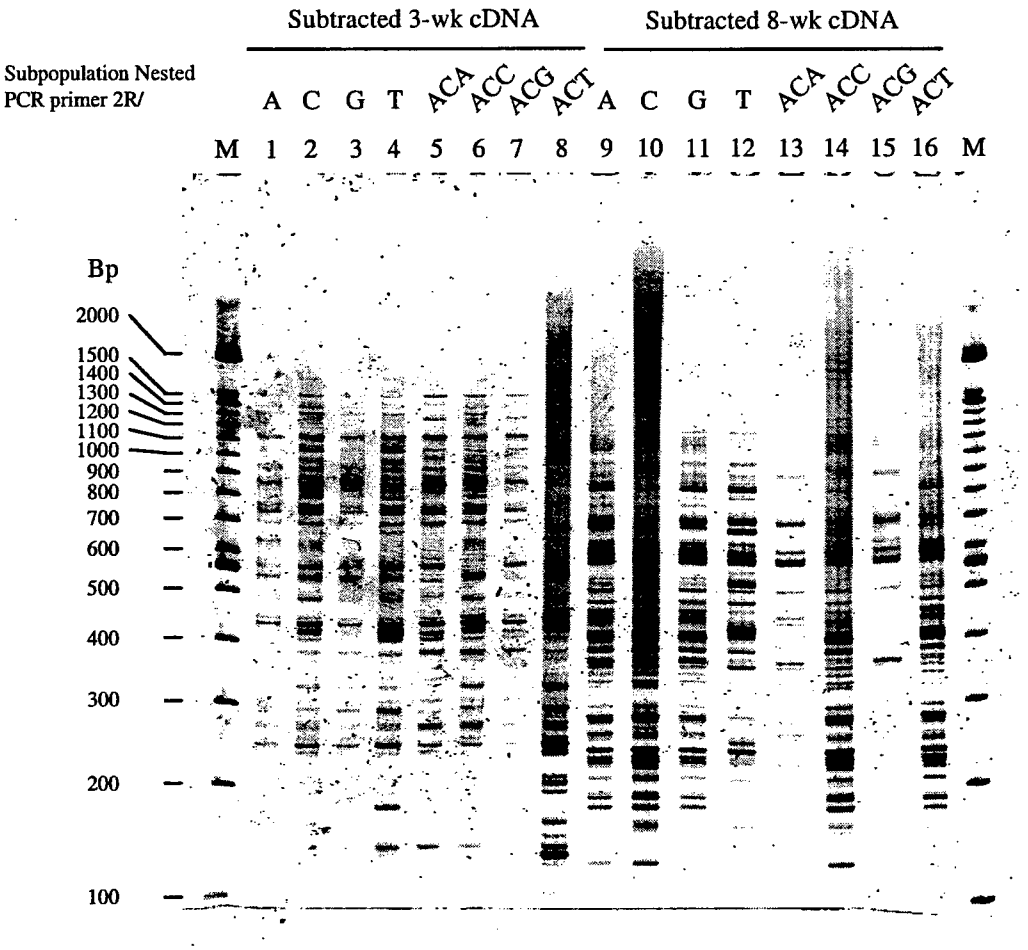
Subtracted 3-wk cDNA
Subtracted 8-wk cDNA
Subpopulation Nested
PCR primer 2R/
A C G T ACA ACC ACG ACT A C G T ACA ACC ACG ACT
M 1 2 3 4 5 6 7 8 9 10 11 12 13 14 15 16 M
Bp
2000
1500
1400
1300
1200
1100
1000
900
800
700
600
500
400
300
200
100

Figure 3

Probe

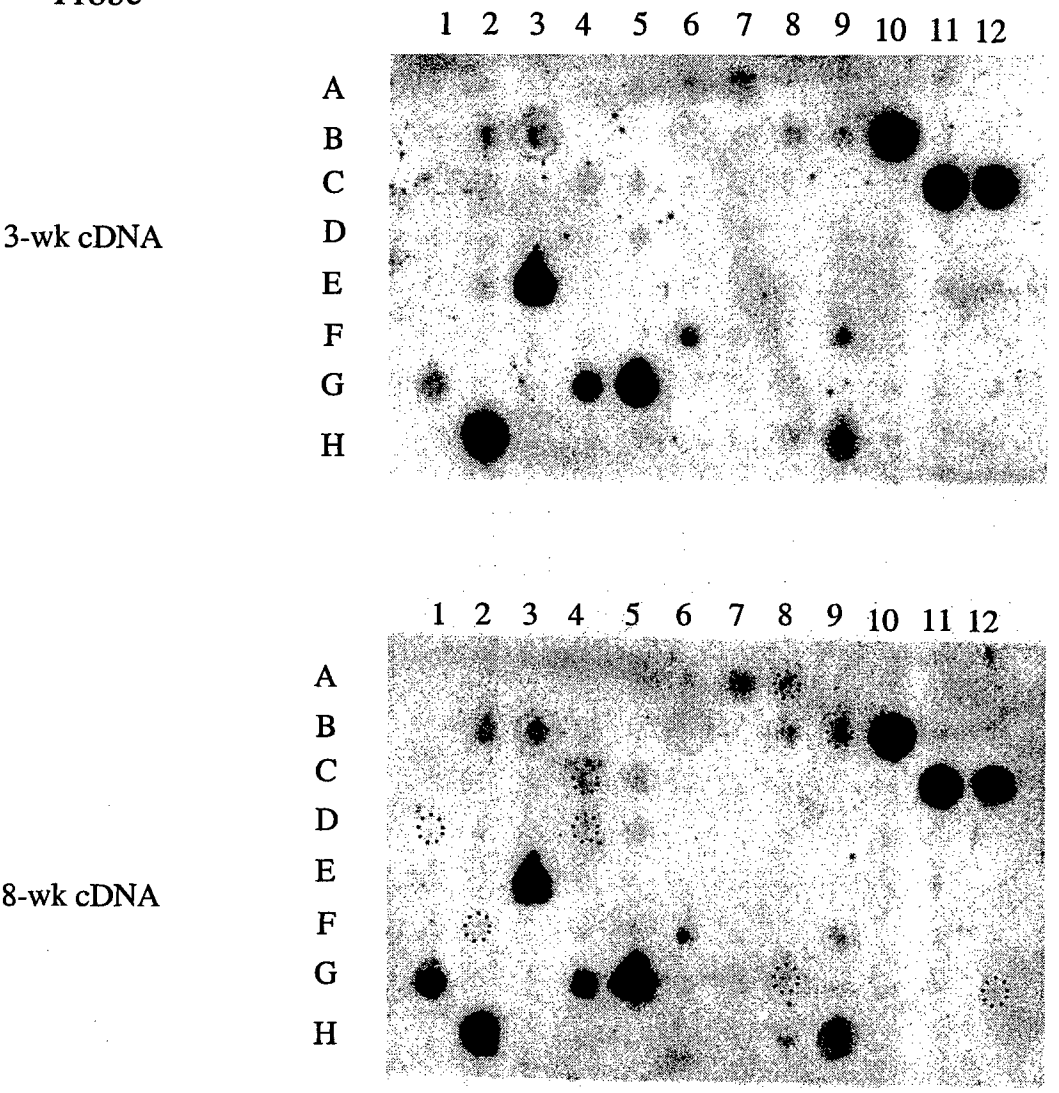

Figure 4

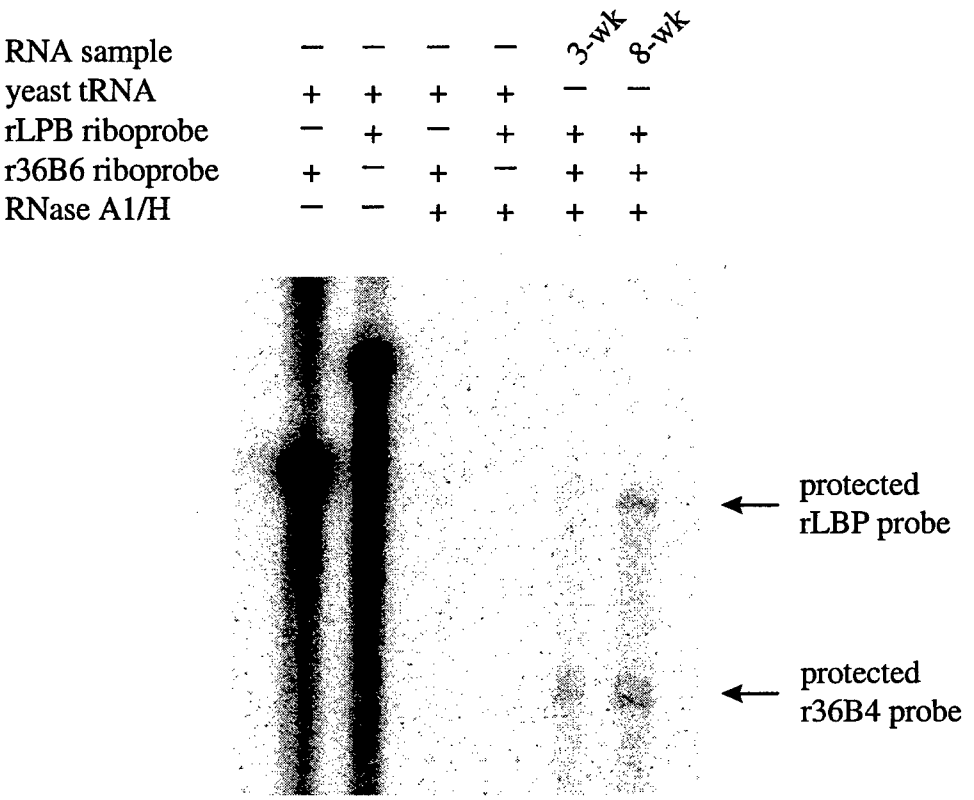
RNA sample
yeast tRNA
rLPB riboprobe
r36B6 riboprobe
RNase A1/H
3-wk
8-wk
protected
rLBP probe
protected
r36B4 probe